

**PNNL-11046**

**UC-810**

**Project Technical Information**

**RECEIVED**

**JUL 15 1997**

**OSTI**

*PVTD-T3B--95-210*

**RECEIVED**

**MAR 28 1996**

---

**Hanford Low-Level Waste Process OSTI  
Chemistry Testing Data Package**

H. D. Smith  
E. M. Tracey  
J. G. Darab  
P. A. Smith

---

**March 1996**

**Prepared for the U.S. Department of Energy  
under Contract DE-AC06-76RLO 1830**

**Pacific Northwest National Laboratory  
Operated for the U.S. Department of Energy  
by Battelle Memorial Institute**



## DISCLAIMER

This report was prepared as an account of work sponsored by an agency of the United States Government. Neither the United States Government nor any agency thereof, nor any of their employees, makes any warranty, express or implied, or assumes any legal liability or responsibility for the accuracy, completeness, or usefulness of any information, apparatus, product, or process disclosed, or represents that its use would not infringe privately owned rights. Reference herein to any specific commercial product, process, or service by trade name, trademark, manufacturer, or otherwise does not necessarily constitute or imply its endorsement, recommendation, or favoring by the United States Government or any agency thereof. The views and opinions of authors expressed herein do not necessarily state or reflect those of the United States Government or any agency thereof.

## **DISCLAIMER**

**Portions of this document may be illegible  
electronic image products. Images are  
produced from the best available original  
document.**

## **Hanford Low-Level Waste Process Chemistry Testing Data Package**

H. D. Smith  
E. M. Tracey  
J. G. Darab  
P. A. Smith

March 1996

Prepared for  
the U.S. Department of Energy  
under Contract DE-AC06-76RLO 1830

Pacific Northwest National Laboratory  
Richland, Washington 99352

## DISCLAIMER

This report was prepared as an account of work sponsored by an agency of the United States Government. Neither the United States Government nor any agency thereof, nor Battelle Memorial Institute, nor any of their employees, makes any warranty, express or implied, or assumes any legal liability or responsibility for the accuracy, completeness, or usefulness of any information, apparatus, product, or process disclosed, or represents that its use would not infringe privately owned rights. Reference herein to any specific commercial product, process, or service by trade name, trademark, manufacturer, or otherwise does not necessarily constitute or imply its endorsement, recommendation, or favoring by the United States Government or any agency thereof, or Battelle Memorial Institute. The views and opinions of authors expressed herein do not necessarily state or reflect those of the United States Government or any agency thereof.

PACIFIC NORTHWEST NATIONAL LABORATORY

*operated by*

BATTELLE

*for the*

UNITED STATES DEPARTMENT OF ENERGY

*under Contract DE-AC06-76RLO 1830*

Printed in the United States of America

Available to DOE and DOE contractors from the  
Office of Scientific and Technical Information, P.O. Box 62, Oak Ridge, TN 37831;  
prices available from (615) 576-8401.

Available to the public from the National Technical Information Service,  
U.S. Department of Commerce, 5285 Port Royal Rd., Springfield, VA 22161



The document was printed on recycled paper.

## CONTENTS

1. List of Tables.....	iv
1. List of Figures.....	vi
1. Introduction.....	1
2. Summary.....	2
3. Literature Review of Denitration Processes.....	3
3.1. Thermal Denitration.....	3
3.2. Chemical Denitration.....	6
3.2.1. Formic Acid and Formaldehyde.....	7
3.2.2. Sugar, Carbon, and Starch.....	9
3.2.3. Glycolic Acid and Citric Acid.....	10
3.3. Denitration Catalysts.....	10
3.4. Thermochemical Denitration.....	11
3.5. Implications to Hanford LLW Processing.....	13
4. Dry-Out and Low-Temperature Calcination of Low-Level Waste Melter Feeds.....	14
4.1. Introduction.....	14
4.2. Experimental Approach.....	16
4.2.1. Materials.....	16
4.2.3. Equipment.....	18
4.2.4. Dry-Out and Calcination Procedures.....	18
4.3. Results and Discussion.....	21
4.3.1. DSSF-Reductant Interactions.....	22
4.3.2. DSSF/Glass Precursor-Reductant Interactions with Glass Precursors.....	24
4.3.2.1. Citric, Glycolic, and Formic Acids.....	24
4.3.2.2. Sugar, Starch, and Carbon.....	30
4.3.2.3. Vendor Feeds.....	38
5. High-Temperature Calcination Test Results on the LLW Baseline, US Bureau of Mines Feed, and Vectra Feed.....	41
5.1. Introduction.....	41
5.2. Experimental.....	41
5.3. Results and Discussion.....	43
6. References.....	47
Appendix Material.....	49

## LIST OF TABLES

Table 4.1.1. Summary of tests performed in this work.....	15
Table 4.2.1.1. Target composition of simulated Hanford double-shell slurry feed (DSSF) waste inventory after pretreatment.....	16
Table 4.2.1.2. Target and actual density and composition of DSSF simulant used in this work. ....	17
Table 4.2.1.3. Glass precursor additives added to 100 grams of DSSF simulant. The target glass composition, after drying and vitrification, is that of LD6-5510 (in wt%57 SiO <sub>2</sub> , 20 Na <sub>2</sub> O, 5 B <sub>2</sub> O <sub>3</sub> , 5 CaCO <sub>3</sub> , 10 Al <sub>2</sub> O <sub>3</sub> , balance minor DSSF waste components).....	17
Table 4.3.1.1. Summary of offgas analysis results obtained from simulant-reductant interaction tests.....	23
Table 4.3.1.2. Summary of the distribution of Re between the slurry supernate and suspended solids before and after the addition of reductant.....	24
Table 4.3.2.1.1. Results of offgas analysis obtained from dry-out/low-temperature calcination tests performed on melter feeds containing formic, glycolic, and citric acids.....	28
Table 4.3.2.1.2. Results of NH <sub>3</sub> offgas analysis obtained from dry-out/low-temperature calcination tests performed on melter feeds containing formic, glycolic, and citric acids.....	29
Table 4.3.2.1.3. Summary of the distribution of Re between the primary and secondary condensers after the dry-out/low temperature calcination of various melter feeds.....	30
Table 4.3.2.2.1. Results of offgas analysis obtained from dry-out/low-temperature calcination tests performed on melter feeds containing sugar and starch.....	35
Table 4.3.2.1.2. Results of NH <sub>3</sub> offgas analysis obtained from dry-out/low-temperature calcination tests performed on melter feeds containing sugar and starch.....	36
Table 4.3.2.1.3. Summary of the distribution of Re between the primary and secondary condensers after the dry-out/low temperature calcination of melter feeds containing various amounts of sugar and starch.....	37

Table 4.3.2.3.1. Results of offgas analysis obtained from dry-out/low-temperature calcination tests performed on the USBM melter feed. ....38

Table 5.3.1. Results of offgas analysis obtained from high-temperature calcination tests performed on DSSF, USBM, and Vectra melter feeds. Maximum volume expansions are also reported. ....43

## LIST OF FIGURES

Figure 4.2.3.1. Schematic diagram of the system used for the dry-out and low-temperature calcination studies in this work.....	19
Figure 4.2.3.2. Off-gas measuring system used in conjunction with dry-out apparatus illustrated in Figure 4.2.3.1.....	20
Figure 4.3.2.1.1. Temperature and offgas profiles as a function of time which resulted from drying the melter feed containing citric acid.....	25
Figure 4.3.2.1.2. Temperature and offgas profiles as a function of time which resulted from drying the melter feed containing glycolic acid.....	26
Figure 4.3.2.1.3. Temperature and offgas profiles as a function of time which resulted from drying the melter feed containing formic acid.....	27
Figure 4.3.2.2.1. Temperature and offgas profiles as a function of time which resulted from the T95-LLW-Sugar(0.5) test.....	31
Figure 4.3.2.2.2. Temperature and offgas profiles as a function of time which resulted from the T95-LLW-Sugar(1.0) test.....	32
Figure 4.3.2.2.3. Temperature and offgas profiles as a function of time which resulted from the T95-SLLW-Sugar(0.5) test.....	33
Figure 4.3.2.2.4. Temperature and offgas profiles as a function of time which resulted from the T95-SLLW-Sugar(0.75) test.....	34
Figure 5.3.1. Temperature and offgas profiles as a function of time which resulted from the USBM-LD6-5510-1400B test.....	39
Figure 5.3.2. Temperature and offgas profiles as a function of time which resulted from the USBM-M1BPW-011P test.....	40
Figure 5.2.1. Schematic diagram of the system used for the high-temperature calcination studies in this work.....	42
Figure 5.3.1. Offgas profiles and normalized sample volume as a function of temperature which resulted during calcination of the DSSF feed at 10°C/min. ....	44
Figure 5.3.2. Offgas profiles and normalized sample volume as a function of temperature which resulted during calcination of the USBM feed at 10°C/min. ....	45

Figure 5.3.3. Offgas profiles and normalized sample volume as a function of temperature which resulted during calcination of the Vectra feed at 10°C/min. ....46

## 1. INTRODUCTION

Recently, the Tri-Party Agreement (TPA) among the State of Washington Department of Ecology, U.S. Department of Energy (DOE) and the US Environmental Protection Agency (EPA) for the cleanup of the Hanford Site was renegotiated. The revised agreement specifies vitrification as the encapsulation technology for low level waste (LLW). A demonstration, testing, and evaluation program underway at Westinghouse Hanford Company to identify the best overall melter-system technology available for vitrification of Hanford Site LLW to meet the TPA milestones. Phase I is a "proof of principle" test to demonstrate that a melter system can process a simulated highly alkaline, high nitrate/nitrite content aqueous LLW feed into a glass product of consistent quality. Seven melter vendors were selected for the Phase I evaluation: joule-heated melters from GTS Duratek, Incorporated (GDI); Envitco, Incorporated (EVI); Penberthy Electromelt, Incorporated (PEI); and Vectra Technologies, Incorporated (VTI); a gas-fired cyclone burner from Babcock & Wilcox (BCW); a plasma torch-fired, cupola furnace from Westinghouse Science and Technology Center (WSTC); and an electric arc furnace with top-entering vertical carbon electrodes from the U.S. Bureau of Mines (USBM).

The chemical behavior of LLW during the conversion to glass is crucial to safety issues, melting rate, and evaluation of commercial vendor technology. More specifically, the behavior of vitrification additives during heating and in the vitrification process must be understood to avoid hazardous hydrogen and/or ammonia generation or the production of environmentally damaging  $\text{NO}_x$ . In addition, the reactions and the associated reaction paths are affected by the batch chemistry and have an effect on the melting rate. Since the melter vendors were permitted to match the batch chemistry to their technology, a general understanding of the conversion of LLW to glass was sought.

To address these issues and fulfill the commitments in the investigation plan (C94-21.04D Rev.1), this report (milestone T3B-95-210) provides the following: (1) a review of denitration literature relevant to LLW; (2) results of slurry evaporation tests as a function of reductant content and supporting tests performed on the US Bureau of Mines (USBM) and Vectra Technologies, Incorporated feeds; (3) calcination test results on the LLW baseline Double Shell Slurry Feed (DSSF), USBM and Vectra feeds; and (4) supporting vitrification tests on selected calcined feeds.

## 2. SUMMARY

- Of all the reductants studied, only formic acid displayed significant reactivity with the Hanford Site Double Shell Slurry Feed (DSSF) simulant at 95°C. Other organic acids showed a very subdued reactivity.
- All the feeds tested displayed an exothermic reaction upon being heated and dried to about 250°C. The feed made up with formic acid displayed the least energetic exotherm, which appeared to be initiated at about 150°C based on the observed offgas evolution.
- All the feeds tested produced H<sub>2</sub> and/or NH<sub>3</sub> when calcined. Formic and glycolic acids produced minimal NH<sub>3</sub> but considerable amounts of H<sub>2</sub> compared to the other reductants studied.
- Very small amounts of rhenium (a surrogate for technetium) were observed in the condensates collected during the dry-out and calcination tests. It is likely that the small amounts observed were transported as aerosols which were observed in association with exothermic activity.
- Compared to the DSSF and USBM feeds, the Vectra feed produced no N<sub>2</sub>O, NO, or H<sub>2</sub> offgases up to 1200°C. These results indicate that the nitrate/nitrite in the LLW feed has been completely mitigated by the Vectra feed processing conditions.
- We also evaluated some of the feeds studied here in terms of their general melt behavior and characteristics at 1350°C (the melting point for the LD6-series glasses of which most of these feeds are formulated after). It is beyond the scope of this report to discuss these results any more than what will be summarized here. In general, however, the several attempts at melting treated feeds that contained added reductants (specifically, the USBM feed and DSSF based feeds treated with various concentrations of reductants) resulted in highly corrosive melts (Pt-10%Rh crucibles were attacked) and final glasses that were black and contained visible metallic particles. Obviously, these feeds are too reducing and, even though the nitrate/nitrite can be mitigated, the feeds are quite useless in terms of producing a durable waste form. The Vectra feed and untreated DSSF feeds, on the other hand produced typically green, optically transparent glasses.

### 3. LITERATURE REVIEW OF DENITRATION PROCESSES

A variety of thermal, chemical, and thermochemical denitration methods are reviewed here. Thermal denitration uses high temperatures (in excess of 500°C) to decompose the nitrate and nitrite compounds in the waste stream. Chemical denitration uses chemical reductants such as formic acid to decompose the nitrates and nitrites while keeping temperatures low (100°C). Finally, thermochemical denitration uses a combination of both methods.

#### 3.1. Thermal Denitration

Thermal decomposition of sodium nitrate and sodium nitrite uses temperatures exceeding 500°C to denitrate waste. A variety of studies have been performed on thermal denitration and various large scale denitration methods currently exist. These thermal denitration methods produce off gases that generally consist of N<sub>2</sub>O, N<sub>2</sub>, O<sub>2</sub>, and NO but the relative amounts are dependent on the test or operating conditions. The relative amount of nitrate or nitrite destruction is also dependent on the test or operating conditions.

The decomposition of NaNO<sub>3</sub> to NaNO<sub>2</sub> is the first step in nitrate decomposition and begins at approximately 500°C (Ryan, 1994; Hoshino et al., 1981; Bond and Jacobs, 1966; Chun, 1977):



The reaction rate is the same for either an oxygen or argon atmosphere (Bond and Jacobs, 1968) and reaches equilibrium within two hours at 700°C (Burger et al., 1973). The reaction is endothermic (Bond and Jacobs, 1966).

The decomposition of sodium nitrite, either as the starting compound or as an intermediate in sodium nitrate destruction, is not as clear. Bond and Jacobs (1966) studied the isothermal decomposition of sodium nitrate between 570°C and 760°C using a thermobalance in flowing (100 ml/min) argon or air. As discussed previously, the authors concluded that the first step in the decomposition of sodium nitrate is the production of sodium nitrite and oxygen. The next step is the decomposition of sodium nitrite. The authors proposed the following reactions:



Relation 3.1.2 was concluded to be the major reaction since only a small amount of NO was formed. Because the reaction products and reaction rates are independent of the atmosphere, the authors concluded that atmospheric oxygen does not participate in the reaction. They proposed a mechanism that involves a superoxide ion as an intermediate. Activation energies and rate equations were also determined for relations 3.1.1 and 3.1.2.

Burger et al. (1976) used the results of the Bond and Jacobs (1966) studies to calculate the time for 90% completion of the  $\text{NaNO}_2$  decomposition as a function of temperature. According to their calculations, at a temperature of  $700^\circ\text{C}$ , it should take 132 minutes for 90% completion and at a temperature of  $850^\circ\text{C}$ , the same reaction should take 9 minutes. Based on these data, it was calculated that heating to  $830^\circ\text{C}$  for a maximum of 30 minutes would be sufficient for complete decomposition of sodium nitrate or sodium nitrite. To verify that heating to  $800^\circ\text{C}$  would be sufficient to decompose sodium nitrate or sodium nitrite, Burger et al. (1973) ran a series of experiments in which 20 g of sodium nitrate was placed in crucibles. The crucibles were held in a furnace set at 700 to  $850^\circ\text{C}$  for times ranging from 100 to 1070 minutes. After 1070 minutes at  $700^\circ\text{C}$ , 65.2% of the original  $\text{NaNO}_3$  remained and after 240 minutes at  $850^\circ\text{C}$  7.1% of the  $\text{NaNO}_3$  remained. These experiments indicated that  $\text{NaNO}_3$  decomposition is much slower and less complete at a temperature of  $800^\circ\text{C}$  than indicated by Bond and Jacobs (1966).

Abe et al. (1983) examined sodium nitrite decomposition in an argon atmosphere at a heating rate of  $5^\circ\text{C}/\text{min}$ . Sodium nitrite was heated to  $600^\circ\text{C}$  and the distribution of the sodium between the reaction products of  $\text{Na}_2\text{O}$ ,  $\text{NaNO}_3$ ,  $\text{NaNO}_2$  was determined. Unlike Bond and Jacobs (1966), the authors reported an effect of the atmosphere on the reaction pathways. In an argon atmosphere, sodium nitrite decomposed at about  $450^\circ\text{C}$  to form equimolar amounts of sodium nitrate and sodium oxide with a concomitant generation of NO. In an oxygen atmosphere, sodium nitrite reacted with  $\text{O}_2$  at about  $400^\circ\text{C}$  to form sodium nitrate, and decomposed to form sodium oxide above  $500^\circ\text{C}$ . The authors proposed the following reactions:



These may be considered as intermediate reactions for the overall destruction of  $\text{NaNO}_2$  to  $\text{Na}_2\text{O}$  and it is expected that heating to higher temperatures would lead to the complete destruction of sodium nitrate and sodium nitrite.

Hoshino, et al. (1980) studied the decomposition of sodium nitrate using thermal analysis, gas analysis, and chemical analysis. Sodium nitrite (80 mg) was weighed in a reaction vessel and was heated to  $900^\circ\text{C}$  at 5 or  $20^\circ\text{C}/\text{min}$ . Argon (50 ml/min) was used as the carrier gas. Unlike Bond and Jacobs (1966), very little  $\text{N}_2$  was formed. Thermal decomposition of sodium nitrate started at  $450^\circ\text{C}$  and the gases formed were  $\text{O}_2$ ,  $\text{NO}$ , and  $\text{N}_2$  ( $\text{N}_2$  only over  $680^\circ\text{C}$ ). The overall decomposition was exothermic. Decomposition started with the production of oxygen and sodium nitrite as discussed above. Relation 3.1.3 was proposed as the main reaction for the decomposition of sodium nitrite which occurred through several possible intermediate reactions involving sodium peroxide.

Sodium peroxide,  $\text{Na}_2\text{O}_2$ , has also been reported to be a possible product of sodium nitrate and sodium nitrite decomposition (Quinn, 1911; Bond and Jacobs, 1966; Hoshino, 1980). Sodium peroxide was reported to begin to decompose at  $280^\circ\text{C}$ , fuse at  $510^\circ\text{C}$  and to exist as a heterogeneous mixture with  $\text{Na}_2\text{O}$  between  $510^\circ\text{C}$  and  $545^\circ\text{C}$ . Above  $545^\circ\text{C}$ , sodium peroxide decomposes to  $\text{O}_2$  and  $\text{Na}_2\text{O}$  (Rode and Golder, 1956). But, Burger et al. (1973) found that it was stable even at high temperatures. Burger et al. (1973) found evidence of  $\text{H}_2\text{O}_2$  in water leaches from holding  $\text{NaNO}_3$  at  $850^\circ\text{C}$  for 4 hours, which indicates the presence of  $\text{Na}_2\text{O}_2$  in the melt. Abe et al. (1983) also proposed that  $\text{Na}_2\text{O}_2$  is formed in the melt under an argon atmosphere but only as an intermediate.

Chun (1977) performed TGA on sodium nitrate (400 mg) with maximum temperature of  $950^\circ\text{C}$  and a heating rate of 3 to  $4^\circ\text{C}/\text{min}$ . Air was used as the carrier gas. Then samples were heated to  $1100^\circ\text{C}$  in the furnace and held for 3 hours. Sodium nitrate began to lose weight at  $588^\circ\text{C}$ . The total weight loss was 93% when heated up to  $1100^\circ\text{C}$  and 67.7 % when heated to  $940^\circ\text{C}$ . The theoretical weight loss assuming all of the sodium nitrate converts to sodium oxide ( $\text{Na}_2\text{O}$ ) is 63.5%. Chun

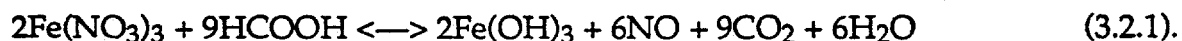
(1977) concluded that the discrepancy between the observed weight loss and the theoretically predicted weight loss was due to the volatilization of sodium nitrate which was previously reported to occur by Newby and Dickerson (1972).

Sodium nitrate and sodium nitrite have also been reported to volatilize by Burger et al. (1973). It was observed that a large fraction of the material vaporized at a temperature of approximately 650°C during their experiments. The solid product that vaporized was mainly sodium nitrite but also contained some sodium nitrate and sodium oxide. The solid that formed in the gas phase was extremely fine and could be carried through several feet of tubing at low gas flow rates.

The use of a plasma torch fired cupola test system was used to denitrate high-level radioactive waste simulant by calcination at Hanford (Gass et al., 1993). Calcination destroyed 95% of the nitrates and nitrites producing off-gases consisting primarily of N<sub>2</sub> and O<sub>2</sub> with low concentrations of NO<sub>x</sub>, CO, and CO<sub>2</sub>. The waste volume reduction was 80%. Temperatures of the crucible ranged from 900 to 1000°C.

### 3.2. Chemical Denitration

Denitration can be performed at lower temperatures through chemical additions to the waste stream. Chemical denitration removes nitrates and nitrites or free nitric acid through the use of one or several reducing agents, such as formic acid. As was the case for thermal denitration, nitrates and nitrites can be chemically decomposed to N<sub>2</sub>, N<sub>2</sub>O, NO, and NO<sub>2</sub>, with the relative amounts of these gases depending on the reductant used and the experimental conditions. Chemical denitration also reduces the amount of nitrates by driving hydrolysis reactions (Orebaugh, 1976). For example:



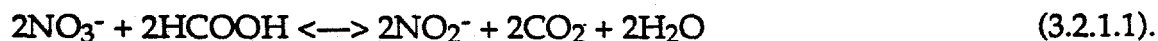
Other easily hydrolyzable cations include mercury and zirconium.

The three most commonly used reducing agents are formic acid, formaldehyde and sugar. Other reducing agents include carbon in its elemental and other forms (coke, coal, graphite, or starch), and other organic compounds such as citric acid, EDTA, and glycolic acid. The degree of denitration depends on the salt content and the amount of hydrolyzable species.

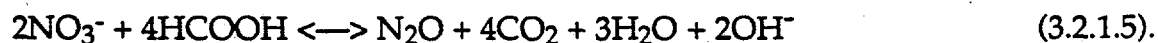
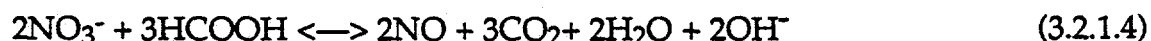
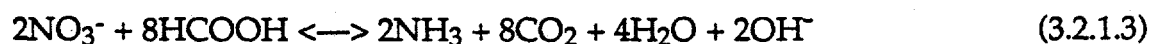
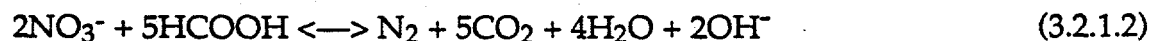
Generally an induction time is present prior to chemical denitration. The four main parameters that influence the induction time are temperature, pressure, respective concentrations, and salt concentration. At room temperatures, induction times ranged from 4 to 10 minutes during chemical denitration in which formic acid was the reductant. Ratios of reducing acid to nitrate ranged from 9.2 to 1.8, respectively (Cecille and Kelm, 1986).

### 3.2.1. Formic Acid and Formaldehyde

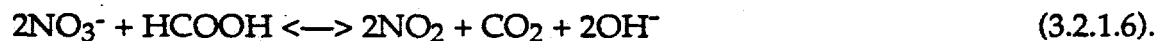
Formic acid has been shown in extensive studies to be an effective reducing agent (Miele and Johnson, 1983; Cox et al., 1992; Brickford et al.; Burril, 1987; Cecille and Kelm, 1986; Holze et al., 1979; Kelm et al., 1980; Kubota et al., 1979; Orebaugh, 1976]. The reactions between formic acid and sodium nitrate are numerous and depend on the acidity of the solution and relative concentrations of the reductant and salt. The stoichiometric reaction between the nitrate anion and formic acid is given by the following relationship (Meile and Johnson, 1983):



When formic acid is in excess, several reactions may occur:



When the formic acid is limited, a different mechanism of denitration occurs:



Similar equations can be written in the acidic form. Formic acid denitration is generally a violent reaction and must be controlled by the rate of acid addition. Excessive foaming has also been a problem. This has been avoided by slowly adding concentrated formic acid into boiling waste solution under a purge of inert gas.

Depending on the relative concentrations of nitrate and the reductant, different off-gases will be produced. Cecille and Kelm (1986) reviewed the addition of formic acid

to boiling nitric acid and sodium nitrate (limited formic acid) and the addition of sodium nitrate and nitric acid to boiling formic acid (excess formic acid). The first scenario gave an off-gas composition of 68% NO, 4% NO<sub>2</sub>, and 28% N<sub>2</sub>O, whereas that of the second consisted of 22% NO, 3% NO<sub>2</sub>, and 75% N<sub>2</sub>O. Carbon dioxide generation was not determined. Denitration rate and reaction mechanisms will also be dependent on temperature, pressure, purge gas, and other compounds in the reaction solution such as noble metals.

Kelm et al. (1980) studied formic acid denitration by adding the waste solution to boiling formic acid and boiling (100 to 102°C) under reflux to form N<sub>2</sub>O and CO<sub>2</sub> as the primary products with 80 to 90% of the nitric acid being decomposed. Waste solutions were added slowly under reflux conditions to a stoichiometric amount of boiling formic acid. The reaction was completed in 3 hours after the final waste addition. Holze et al. (1979) also studied the addition of waste solutions containing nitric acid to boiling formic acid. From their work, kinetic expressions valid for a wide range of concentrations were established. These kinetic studies indicated that scheme 3.2.1.5 was predominant over most of the reaction, with scheme 3.2.1.4 becoming more significant towards the end of the reaction.

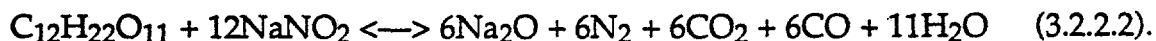
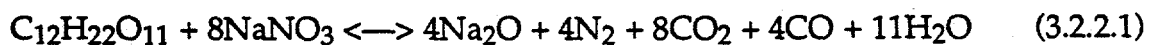
Several studies have shown that increasing the salt content improves the denitration rate and decreases the induction time in acidic waste solutions. Cecille and Kelm (1986) determined that the last 20% of nitric acid will be destroyed very slowly in the presence of formic acid. With sodium nitrate, the reaction will be completed in 2 hours. Kubota et al. (1979) examined the effects of nitrite addition to the denitration process. The nitrite addition reduced the induction period to almost zero and the maximum gas evolution rate to less than 60% of that obtained in the absence of nitrite. Induction times for denitration with formic acid can be reduced to a few seconds by adding sodium nitrite and operating at the boiling point of the system (Cecille and Kelm, 1986; and Kubota et al., 1979). The addition of sodium nitrite also reduces the maximum gas evolution rate (Kubota et al., 1979).

Cox et al. (1992) reported thermochemical nitrate destruction at high temperature (300 to 350°C) under basic conditions in a batch reactor using formate as the reducing agent. Three moles of formate were added per mole of nitrate. After 2 hours of digestion it was found that 74-99% of the original nitrate was destroyed, with N<sub>2</sub>O and N<sub>2</sub> being detected in the offgas.

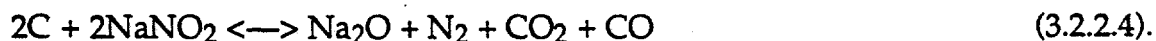
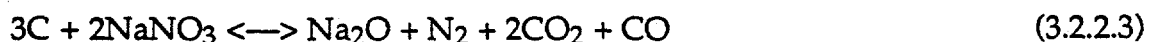
Formaldehyde denitration has also been extensively studied. (Miele and Johnson, 1983; Cecille and Kelm, 1986; Evans, 1959; Frosman and Oberg, 1963) An intermediate in the formaldehyde denitration is formic acid; therefore, the reaction pathways for formic acid and formaldehyde denitration are similar. The resulting off-gases for formic and formaldehyde are also practically identical (Cecille and Kelm, 1986).

### 3.2.2. Sugar, Carbon, and Starch

Sugar has also been shown to be an effective reducing agent (Miele and Johnson, 1983; Cox et al., 1992; Bray and Martin, 1962; Coppinger, 1963; MacDougall et al., 1982). The decomposition of nitric acid is linearly dependent on the concentration of sugar. Due to the relatively slow rate of reaction, which does not give rise to foaming, a simple uncomplicated reaction vessel design is possible. Sugar is also a cheaper reductant than formic acid or formaldehyde. Decomposition of nitrate and nitrite by sugar occurs by the follow reactions:



Carbon can also be introduced into the system in the form of elemental carbon or starch. Elemental carbon decomposes nitrate and nitrite by the following reactions:



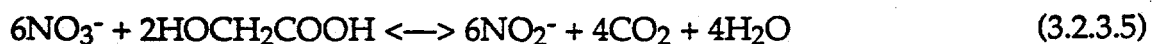
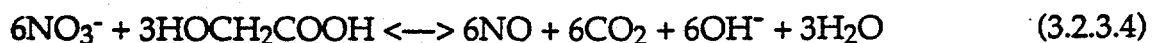
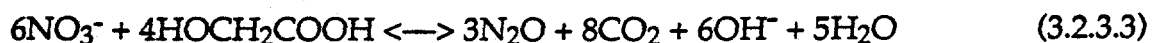
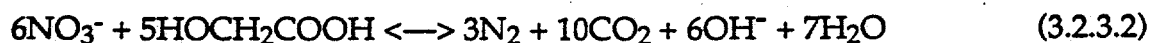
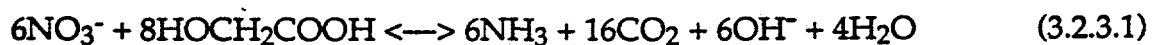
The use of carbon-containing reducing agents to react with nitrate and nitrite at temperatures below their normal thermal decomposition temperatures (i.e.  $\approx 800^\circ\text{C}$ ) will increase the total gas evolved (due to the reductant addition) and will convert the alkali metal nitrates and nitrites to carbonates (Ryan, 1994).

Sugar was investigated as an alternate reductant for the acidic waste in the Purex pilot plant (Bray, 1962). In laboratory studies, sucrose, fructose, glucose, and crude syrups rapidly and controllably decomposed  $\text{HNO}_3$  in aqueous solutions at  $85^\circ\text{C}$ . Approximately 12 to 20 moles of  $\text{HNO}_3$  are destroyed per mole of sucrose. In pilot scale studies performed by Coppinger (1963), sugar was added continuously to hot waste at  $100^\circ\text{C}$  and the solution was digested for 12 hours. Twenty moles of nitric

acid were destroyed per mole of sugar. The reaction proceeded smoothly and was easily controlled. An induction period of 6 minutes was also observed. The addition of nitrite did not reduce the induction period.

### 3.2.3. Glycolic Acid and Citric Acid

Glycolic acid has been used as a reducing agent in the treatment of high-level waste (Smith). Glycolic and citric acids behave similarly to formic acid. Formic acid supplies 2 reducing electrons per mole, while glycolic acid provides 6 electrons per mole. Possible reactions involving glycolic acid with nitrate include the following:



Complexing agents, such as citric acid, have been found to be effective as reducing agents in the presence of radiation (Bray and Martin). Similar reactions as those listed above occur with citric acid, although 18 reducing electrons per mole are involved.

### 3.3. Denitration Catalysts

Some work has been done using catalysts to improve the rate of denitration. Iron has been shown to catalyze denitration with formic acid, formaldehyde and sugar (MacDougall, 1981). Nitric acid (6 M, 500 mL), with and without iron, were added to a reaction vessel and heated to 100°C. The iron content was varied from 0 to 0.2 M Fe(III). Sucrose (2.5 M, 50 mL) was added to the reaction vessel at a rate of 10 mL/min. The number of moles of acid reacting with 1 mole of carbon remained constant with increasing iron content but the reaction rate increased with increasing iron content. At 110°C, however, the rate of denitration was found to be invariant with respect iron concentration.

Meile and Johnson (1984) examined the effectiveness of copper, zinc, platinum, nickel, rhodium, iron oxide, aluminum oxide, and aluminosilicate to act as catalysts in the denitration process. Nickel and copper were tested in the form of metal

turnings, platinum and rhodium as wire, zinc as shot, iron oxide as pellets, aluminum oxide as small spheres, and zeolon as extruded pellets. These forms of catalysts may not be of the most optimal form, but were used in their experiments nonetheless. Denitration was carried out using sodium nitrate and a reductant in a 1:1 ratio. The solution was then evaporated to dryness. Although the results of these catalyst tests were not normalized with respect to catalyst surface area, moisture content, etc., nickel was reported to be the most effective catalytic material.

Brickford et al. (1991) studied denitration and  $\text{NO}_x$  evolution in the use of formic acid as a mercury-reducing agent. Under certain conditions the presence of transition or noble metals resulted in significant formic acid decomposition, with associated  $\text{CO}_2$  and  $\text{H}_2$  evolution:



Saum (1981) demonstrated that the acceleration of denitration in the presence of noble metals is marginal, leading to the production of ammonia through the reaction:



Sugiyama and Takahashi (1967) studied effect of various metal oxides on  $\text{NaNO}_3$  and  $\text{NaNO}_2$  decomposition. They reported significantly altered gas ratios and lower decomposition temperatures in the presence of small amounts of  $\text{V}_2\text{O}_5$ ,  $\text{NiO}$ ,  $\text{ZnO}$ ,  $\text{CoO}$ , or  $\text{MgO}$ .

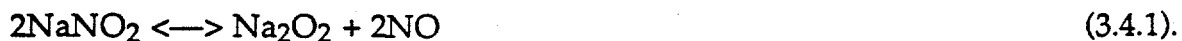
### 3.4. Thermochemical Denitration

In the thermochemical denitration experiments performed by Ray or Ogg (1956), a mixture of various amounts of potassium nitrite and nitrate, chromic oxide, and ferric oxide was heated to slightly above  $300^\circ\text{C}$ . As the potassium nitrate level was reduced the gas collected contained increasing amounts of nitrogen and nitrous oxide. Material containing no potassium nitrite reacted to give 7% nitrogen, 15% nitrous oxide, and the balance nitric oxide. Kozlowski and Bartholomew (1968) studied the reactions of  $\text{NaCOOH}$  and  $\text{NaC}_2\text{H}_3\text{O}_2$  with  $\text{NaNO}_2$  and  $\text{NaNO}_3$  by dropping the  $\text{NaCOOH}$  and  $\text{NaC}_2\text{H}_3\text{O}_2$  into the sodium nitrate or sodium nitrite (50

mg) melt held at 330°C using an argon purge gas. Nitrous oxide was determined to be one of the reaction products.

Hoshino, et al. (1980) studied the effects of several oxides on the decomposition of sodium nitrate using thermal analysis, gas analysis, and chemical analysis. Less than 80 mg of sample was heated in a reaction vessel to 900°C at 5 or 20°C/min. Argon (50 ml/min) was used as the carrier gas. In the presence of SiO<sub>2</sub>, TiO<sub>2</sub>, and ZrO<sub>2</sub>, no N<sub>2</sub> was formed and the reaction peak was narrow, indicating a relatively fast reaction. Nitrogen production increased and the decomposition occurred more slowly in the presence of Al<sub>2</sub>O<sub>3</sub> and MgO. For the NaNO<sub>3</sub> decomposition without the presence of oxides, the reaction is exothermic and N<sub>2</sub> is also produced. In the presence of SiO<sub>2</sub> (at 700°C), TiO<sub>2</sub> (at 640°C), and ZrO<sub>2</sub> (at 690°C), the reactions are endothermic.

Abe et al. (1983) examined sodium nitrite destruction in the presence of silica using TGA-DTA with a GC. A mixture of silica and sodium nitrite (6.9 to 66.9 mg) containing 0.1 mmoles or 0.2 mmoles of sodium nitrite was placed in a platinum vessel using Ar or O<sub>2</sub> as the purge gas (50 ml/min). The samples were heated to 800°C at 5 to 20°C/min after holding at 250°C for one hour to remove the adsorbed water. Sodium nitrite decomposed above 400°C generating only NO, and above 500°C, generating NO, O<sub>2</sub>, sodium nitrate, sodium metasilicate, and disodium disilicate. Results indicated that sodium peroxide forms and is stable in an argon atmosphere at temperatures below 530°C:



Silicates and sodium nitrate formed between 530 and 600°C. Above 600°C, the reaction is identical with that of sodium nitrate with silica because the main species in the melt is sodium nitrate. As the proportion of silica was increased, decomposition temperature decreased and the activation energy increased.

Meile and Johnson (1984) examined two types of thermal denitration processes: one involving a high-temperature fluid wall reactor (HTFWR) and another involving a carbon-nitrate reaction in a molten salt reactor. In the HTFWR, at temperatures of 2200°C and in the presence of carbon black, 96% of the original nitrate was destroyed and no NO<sub>2</sub> was detected in the products. In the absence of the carbon black, only

80% of the nitrate was decomposed. In the molten salt reactor at 1000°C, a 99% reduction of nitrate occurred, generating low but detectable concentrations of NO<sub>x</sub> (100 to 500 ppm).

Thermochemical denitration has been examined by Cox et al. (1992). Cox reported thermochemical nitrate destruction in a high temperature (350°C) batch reactor under basic conditions using glucose as the reducing agent. It was determined that glucose destroyed 48% of the nitrate. N<sub>2</sub>O and NH<sub>3</sub> were not detected in the off-gas.

### 3.5. Implications to Hanford LLW Processing

Hanford Site LLW is characterized by high nitrate and nitrite concentrations. Nitrogen-containing offgas products will thus naturally be of concern during LLW vitrification operations. For example, NO<sub>x</sub> is environmentally damaging and can affect the volatility of certain radionuclides via gas-phase entrainment during vitrification; NH<sub>3</sub> in the offgas can lead to problems associated with inflammability.

Thermal denitration destroys sodium nitrate and sodium nitrite using temperatures in excess of 500°C. The reaction paths and the relative concentrations of offgas products as well as the percent destruction of the sodium compounds are dependent on the test and operating conditions. For example, the presence of oxides as well as the material of the reaction vessel can change the reaction paths. Generally, decomposition begins above 400°C and the off gas products are NO, N<sub>2</sub>, and O<sub>2</sub> and sometimes N<sub>2</sub>O. Sodium nitrate and nitrite have also been shown to be volatile. Denitration can be carried out thermally but temperatures over 800°C are required for the reaction to approach completion. Generally, 80% to 95% of the nitrate is destroyed without presence of a reductant.

The denitration temperature can be lowered and the reaction pathways can be altered through the use of thermochemical denitration. Through the action of added reductants, for example, the distribution of nitrogen-containing offgas products can be altered to contain a greater abundance of reduced (and environmentally benign) products such as N<sub>2</sub>.

## 4. DRY-OUT AND LOW-TEMPERATURE CALCINATION OF LOW-LEVEL WASTE MELTER FEEDS

### 4.1. Introduction

The objective was to provide a preliminary assessment of the process chemistry of dry-out and low-temperature calcination for several reductant types and concentrations. Some of the more important aspects of this assessment and questions to be answered included the following:

1) Gas composition and generation rate (including water loss). It is important to identify toxic, flammable, and/or explosion hazard species so that the plant off-gas system can be designed to mitigate the hazards associated with them. In addition, it is important to know the rate of gas generation so that the dry-out and calciner systems will not over pressurize during operation. This information was gathered as a function of time and temperature.

2) Moisture content. The removal of water is a primary consumer of energy during the dry-out and calcination process. Also, it is important to correlate water loss with the rheological properties of the feed.

3) Enthalpy changes. What endotherms or exotherms are associated with the dry-out or calcination of the feed? What are their magnitudes?

4) General observations such as color changes, phase separation, etc. These observations were taken as part of the test record and are correlated with the other properties measured during this study.

5) Redox properties of the melt produced from the calcine. The primary interest here is the retention of rhenium (a technetium surrogate) during the melting process.

A summary of all the tests completed is indicated in Table 4.1.1. The table also indicates the reductant-to-oxidant ratio, the oxidant content relative to the target value, and the glass precursor components used for producing a high temperature melter feed. Note that tests were also completed with sugar in waste simulant with target levels of oxidant.

The parametric study of the effect of reductants on the processing and vitrification of DSSF simulant was designed with the following questions in mind:

1) Do water soluble hydrocarbons show equivalent reduction capacity in terms of reduction power per hydrogen/carbon electron available for reduction?

Table 4.1.1. Summary of tests performed in this work.

Test	Reductant	[NO <sub>2</sub> <sup>-</sup> ]+[NO <sub>3</sub> <sup>-</sup> ] (% of target)	[Reducing C]/ ([NO <sub>2</sub> <sup>-</sup> ]+[NO <sub>3</sub> <sup>-</sup> ])
<i>DSSF-only feeds (solutions)</i>			
LLW dry-out	none	66	NA
TI-RA-#1-HCOOH	formic acid	66	1.5
TI-RA-#1-Glycolic	glycolic acid	66	1.5
TI-RA-#1-Sugar	sugar	66	2.0
T95-RA-#2-Carbon	carbon black	66	NA
T95-RA-#2-Starch	corn starch	66	1.5
T95-RA-#2-Citric	citric acid	66	1.5
<i>DSSF/glass precursors feeds (slurries)</i>			
T95-LLW-1-HCOOH	formic acid	66	1.5
T95-LLW-1-Glycolic	glycolic acid	66	1.5
T95-LLW-1-Sugar	sugar	66	2.0
T95-LLW-2-Sugar(1.0)	sugar	66	1.5
T95-LLW-Sugar(0.5)	sugar	66	0.76
T95-LLW-2-Citric	citric acid	66	1.5
T95-LLW-Sugar(0.75)	sugar	66	0.75
T95-LLW-Starch(1.0)	corn starch	66	1.5
T95-SLLW-Sugar(0.5)	sugar	100	0.50
T95-SLLW-Sugar(0.75)	sugar	100	0.75
T95-SLLW-Sugar(1.0)	sugar	100	1.0
<i>Melter vendor feeds</i>			
USBM-LD6-5510-1400B	none	NA	1.00-1.25
USBM-M1BPW-011P	none	NA	1.00-1.25

NA = not applicable or not available

2) How sensitive are the redox reactions to the oxidant - reductant ratio in the LLW system?

3) To what extent are H<sub>2</sub> and NH<sub>3</sub> produced during this kind of processing and how is it affected by the use of different reductants?

4) Is rhenium transported (e.g., as a aerosol) during this processing and if so, how much and under what conditions?

For discussion purposes, the standard reactions (relations 3.2.2.1-3.2.2.4) between nitrates and nitrites and carbon or sugar are assumed to be good examples of the

exothermic reactions observed. It is further assumed that many side reactions (alternate reaction pathways) can also occur because of the heterogeneous nature of the dried feed. Hence, there is a potential for variability that we must consider in drawing any conclusions. Side reactions are indicated by other gases in the offgas stream such as:  $\text{NO}_x$ ,  $\text{N}_2\text{O}$ ,  $\text{H}_2$ ,  $\text{CH}_4$ , or  $\text{NH}_3$ . These gases were observed in all the tests to some degree showing that side reactions did indeed occur.

## 4.2. Experimental Approach

### 4.2.1. Materials

The simulant used for this work was based on the target composition given in Table 4.2.1.1 for the 10M  $\text{Na}^+$  Double Shell Slurry Feed (DSSF) LLW inventory. It was

**Table 4.2.1.1. Target composition of simulated Hanford double-shell slurry feed (DSSF) waste inventory after pretreatment.**

Component	Concentration (moles/L)	Compound used in formulation
$\text{Al}(\text{OH})_4^-$	1.0	$\text{Al}(\text{NO}_3)_3 \cdot 9\text{H}_2\text{O}$
$\text{Ca}^{2+}$	0.0010	$\text{Ca}(\text{NO}_3)_2 \cdot 4\text{H}_2\text{O}$
$\text{Cr}(\text{OH})_4^-$	0.0087	$\text{Cr}(\text{NO}_3)_3 \cdot 9\text{H}_2\text{O}$
$\text{Fe}^{3+}$	0.00077	$\text{Fe}(\text{NO}_3)_3 \cdot 9\text{H}_2\text{O}$
$\text{K}^+$	0.50	KOH
$\text{Mg}^{2+}$	0.0010	$\text{Mg}(\text{NO}_3)_2 \cdot 6\text{H}_2\text{O}$
$\text{Mn}^{2+}$	0.00042	$\text{Mn}(\text{NO}_3)_2$
$\text{MoO}_4^{2-}$	0.017	$\text{NaMoO}_4 \cdot \text{H}_2\text{O}$
$\text{Na}^+$	10.0	$\text{NaNO}_3$
$\text{Sr}^{2+}$	0.017	$\text{SrCl}_2$
$\text{Cs}^+$	0.017	$\text{CsNO}_3$
$\text{PO}_4^{3-}$	0.043	$\text{NaH}_2\text{PO}_4 \cdot \text{H}_2\text{O}$
$\text{IO}_3^{3-}$	0.017	$\text{NaIO}_3$
$\text{CO}_3^{2-}$	0.27	$\text{Na}_2\text{CO}_3$
$\text{Cl}^-$	0.16	$\text{NaCl}$
$\text{F}^-$	0.25	$\text{NaF}$
$\text{SO}_4^{2-}$	0.043	$\text{Na}_2\text{SO}_4$
$\text{NO}_3^-$	3.1	$\text{NaNO}_3$
$\text{NO}_2^-$	1.7	$\text{NaNO}_2$
$\text{OH}^-$	3.8	$\text{NaOH}$
TOC	1.4	$\text{Na}_4\text{EDTA} \cdot 2\text{H}_2\text{O}$

**Table 4.2.1.2. Target and actual density and composition of DSSF simulant used in this work.**

Item	Target	Actual
Density (g/mL)	1.4	1.35
[Na <sup>+</sup> ] (mol/L)	10.0	8.35
[NO <sub>2</sub> <sup>-</sup> ] (mol/L)	1.7	1.06
[NO <sub>3</sub> <sup>-</sup> ] (mol/L)	3.1	2.12
[OH <sup>-</sup> ] (mol/L)	3.8	3.6
[Re] (g/L)	3.17	3.17

previously observed that the hydroxide level for the simulant was low and was therefore shimmed to target levels. This shimming was subsequently shown to be wrong and that the nitrate, nitrite, and sodium concentrations were still lower than target levels (Table 4.2.1.2). When the nitrate and nitrite concentrations were shimmed correctly, the sodium was found to be at its correct target level. For this reason, some of tests described here were performed using DSSF simulant with approximately 66% of the target amounts of nitrate and nitrite. In addition, rhenium (3.17 g/L), in the form of ammonium perrhenate (NH<sub>4</sub>ReO<sub>4</sub>), was added to the simulant.

The reductants used in this work included the organic acids formic, glycolic, and citric as well as sugar, corn starch, and carbon black. Glass precursor additives, which are required to be added to the DSSF simulant to bring the final glass composition to specification (glass LD6-5510), included quartz (SiO<sub>2</sub>), aluminum oxide (Al<sub>2</sub>O<sub>3</sub>), boric acid (H<sub>3</sub>BO<sub>3</sub>), and calcium carbonate (CaCO<sub>3</sub>). The amounts of each of these glass precursors required for 100 grams of DSSF simulant are summarized in Table 4.2.1.3.

**Table 4.2.1.3. Glass precursor additives added to 100 grams of DSSF simulant. The target glass composition, after drying and vitrification, is that of LD6-5510 (in wt%: 57 SiO<sub>2</sub>, 20 Na<sub>2</sub>O, 5 B<sub>2</sub>O<sub>3</sub>, 5 CaCO<sub>3</sub>, 10 Al<sub>2</sub>O<sub>3</sub>, balance minor DSSF waste components)**

Additive	Amount (g)
SiO <sub>2</sub>	63.00
Al <sub>2</sub> O <sub>3</sub>	9.83
H <sub>3</sub> BO <sub>3</sub>	9.87
CaCO <sub>3</sub>	7.36

Two additional low temperature calcining tests were run on DSSF-based melter feed simulants. The feed was supplied by the U. S. Bureau of Mines at Albany, Oregon (USBM feed) and was formulated to have the same waste to glass components ratio that were used for the tests in this study. The reductant loading in the USBM feed was 100% of that calculated to completely decompose the nitrates and nitrites. The reductant consisted of 25% of the sugar and 75% of the carbon theoretically required to complete the oxidant decomposition. The feed was manufactured in the form of small pellets at the USBM and was tested at PNL as-received.

#### 4.2.3. Equipment

The system used for the dry-out and low-temperature calcination studies (up to 500°C) on the simulant materials is shown in Figure 4.2.3.1. It consisted of a 2-L Pyrex kettle placed in a temperature controlled heating mantle. The Pyrex kettle lid was modified to accept several thermocouples, a series of condensers, and a divided sweep gas inlet. The sweep gas (argon with a helium tracer) carried off-gas from the reaction vessel plenum, through the condensers to the off-gas measuring system (Figure 4.2.3.2). Three thermocouples were placed in the reaction vessel to detect temperature gradients.

Real time monitoring capabilities were employed to characterize the generation rates of the major gaseous reaction products. The emission rate behaviors of H<sub>2</sub>, CO<sub>2</sub>, N<sub>2</sub>O, CO, O<sub>2</sub>, and N<sub>2</sub> were monitored using a gas chromatograph (GC). A Chemiluminescent NO/NO<sub>x</sub> analyzer was used to measure NO<sub>x</sub>. The nominal sampling cycle time of the GC was approximately 90 s, while that of the NO<sub>x</sub> analyzer was 60 s. A Fourier transform infrared (FTIR) spectrometer was also used to analyze gas samples on an approximately 3 minute cycle time. FTIR provided a backup analysis for each of the above gases (except for O<sub>2</sub>, N<sub>2</sub>, and H<sub>2</sub>) plus detection capabilities for NH<sub>3</sub> and other IR-sensitive gaseous species, such as volatile organics and cyanide.

#### 4.2.4. Dry-Out and Calcination Procedures

The dry-out and calcination laboratory processing and characterization methods were as follows:

- 1) 200-400 mL of prepared melter feed solution or slurry was placed in the reaction vessel. The sweep gas flow was established through the plenum of the reaction

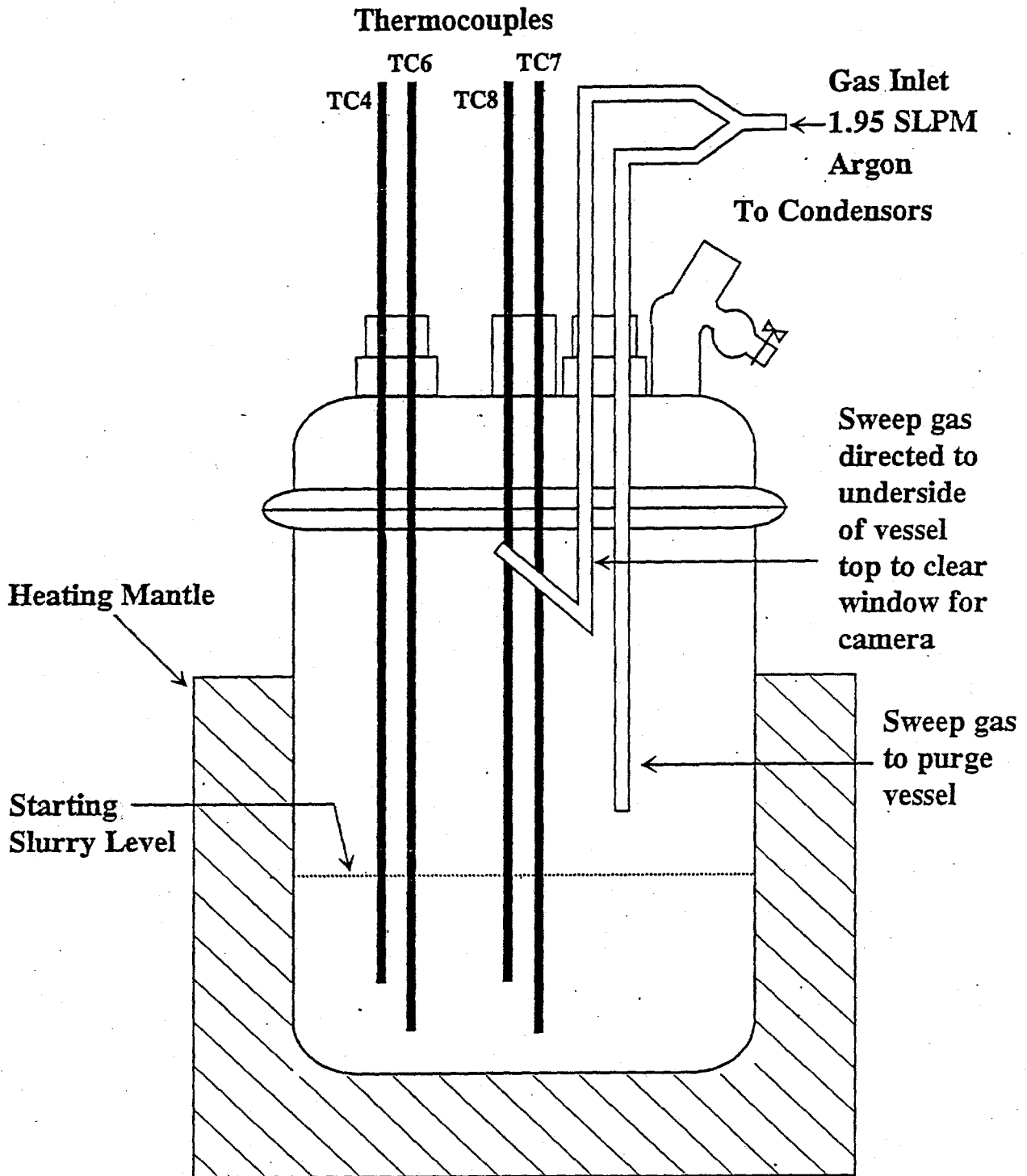
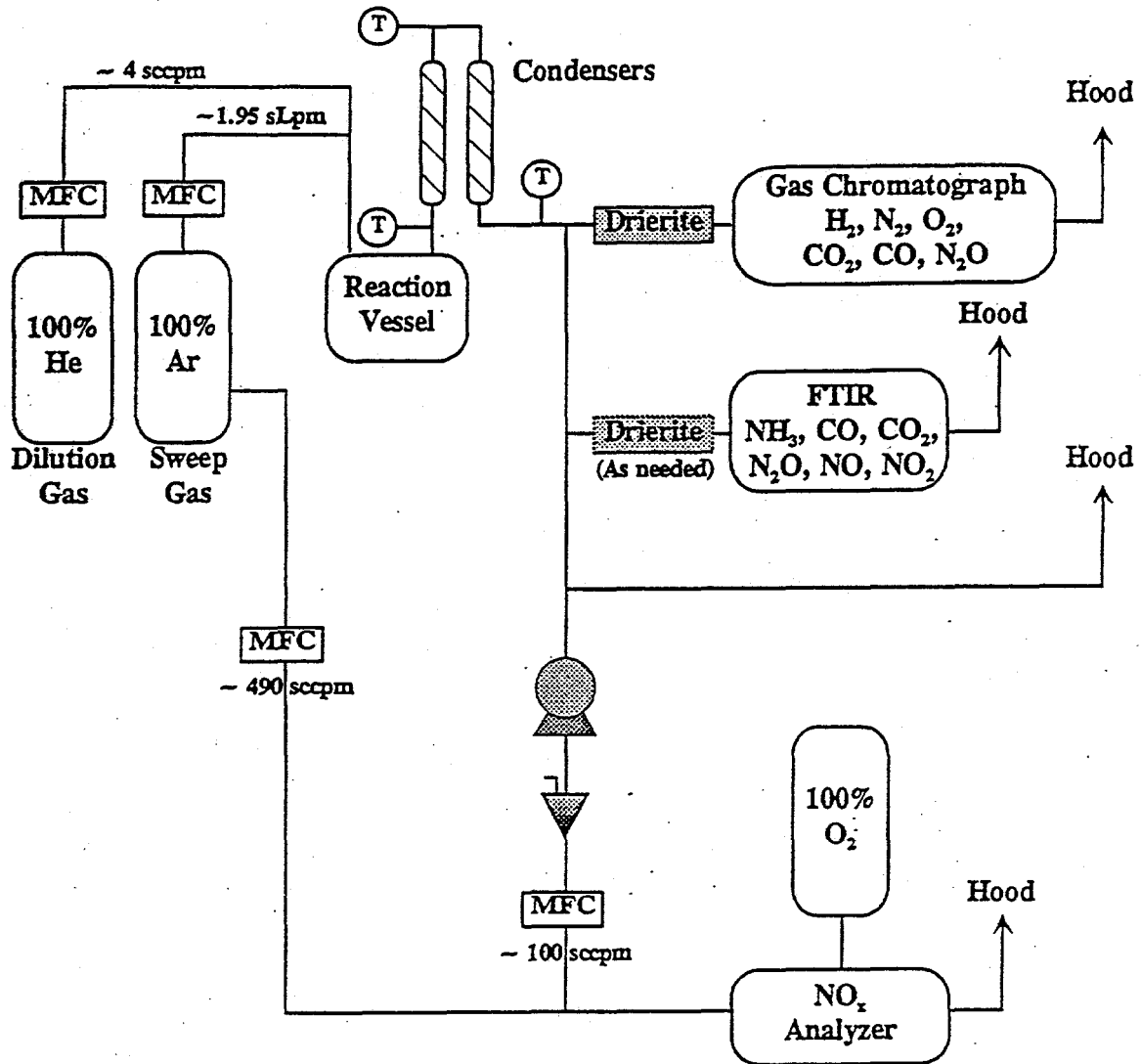


Figure 4.2.3.1. Schematic diagram of the system used for the dry-out and low-temperature calcination studies in this work.



- MFC Mass Flow Controller
- T Temperature Probe
- Metal Bellows Pump
- Needle Valve

<u>Detection Limits</u>		
NO <sub>x</sub> Analyzer	NO <sub>x</sub>	1 ppm
	GC	
	H <sub>2</sub>	10 ppm
	N <sub>2</sub>	100 ppm
	O <sub>2</sub>	100 ppm
	CO <sub>2</sub>	50 ppm
	CO	200 ppm
	N <sub>2</sub> O	50 ppm

Figure 4.2.3.2. Off-gas measuring system used in conjunction with dry-out apparatus illustrated in Figure 4.2.3.1.

vessel (1.95 L per min). The video camera was turned on and positioned to record the slurry surface appearance as viewed through the reaction vessel lid.

2) The appropriate amount of reductant to obtain the desired theoretical reductant-to-oxidant ratio was added to the solution or slurry.

3) The slurry was heated in a step-wise fashion using thermocouple #4 as the control thermocouple. The temperature was allowed to reach a maximum for a given control setting and then the control point was reset to 5°C above the maximum temperature attained at the previous control value. For these tests the temperature was set first to 100°C. Typically there was a thermal overshoot of several degrees, so the temperature set point was usually incremented by 8°- 12°C. This procedure was continued until the slurry was dry. The temperature increments were then increased to 20°C (the set point was increased by 25-30°C). This routine was continued until the temperature attained at the center of the reaction vessel attained about 350°C or an exotherm occurred and elevated the temperature above 350°C. If no exotherm occurred, the temperature was held for 20 to 30 minutes, then the power was turned off. Otherwise the temperature was allowed to return to around 300-350°C before turning off the power.

4) Coincident with the above heating, the temperatures were recorded at 1 to 3 minute intervals and the off-gas was analyzed as described in the previous section. Measured amounts of condensate were taken at regular time intervals. In addition an observation log was kept which also recorded the times at which the set point for the mantle heater was changed.

#### 4.3. Results and Discussion

In general, most of the tests followed a similar course. Starch- and carbon-treated simulant presented special problems which will be discussed in later sections. For the majority of the tests, the simulant mass would first solidify starting at the vessel-simulant interface and proceed inward. The simulant temperature would remain relatively low (<150°C) while significant water was being driven off (>1 g/min). Subsequently, the temperature would rise more rapidly (as fast as the heating mantle could heat it). When the temperature reached 200-250°C all of the organic treated simulant batches displayed a significant exothermic reaction accompanied with greatly increased (several orders of magnitude) off-gas evolution. During this

exothermic period, a "burn front", accompanied by light and smoke emissions, was observed. An aerosol formed during the exothermic reaction and was observed in the ammonia bubbler trap. This indicated that the aerosol was stable enough to travel through several feet of quarter inch tubing. Completion of the exothermic event was indicated by a sudden change from heating at rates as high as hundreds of degrees centigrade per minute to cooling conditions.

Starch-treated feeds presented a special problem in that a highly viscous liquid formed. The resulting slurry did not heat as uniformly as the other slurries where fluid motion helped to maintain a more even temperature distribution. Carbon-treated feeds presented a wetting problem. The one test involving "carbon" as an additive was completed with ground up activated charcoal pellets that contained greater than 50 wt% ash.

The final product of most of these tests was a gray to black, highly porous, brick-like material. The final color depended on the amount of reductant used, with the more reduced materials appearing black (due to the presence of residual carbon?) and the least reduced appearing gray (little or no residual carbon?).

#### 4.3.1. DSSF-Reductant Interactions

These scoping tests were set up to investigate the degree of interaction between the LLW simulant and the reductants under boiling conditions. The primary objective of these tests was to assess the potential hazards of proceeding with more rigorous investigations because the interaction under test conditions had not yet been documented.

The offgas results from these interaction tests are shown in Table 4.3.1.1. The results show that only HCOOH displayed any significant interaction with the simulant, producing CO<sub>2</sub>, NO, and N<sub>2</sub>O, but no H<sub>2</sub>. Based on the amount of CO<sub>2</sub> generation, the relative reactivities of citric acid and glycolic acid were about 20 and 100 times less than that of HCOOH, respectively. Sugar, starch, and carbon were all about four orders of magnitude less reactive than HCOOH. For all of these systems very little H<sub>2</sub> was generated. No methane was detected in this series of tests. We concluded from these results that we could safely add these reductants to the simulated waste prior to the dry out tests.

**Table 4.3.1.1. Summary of offgas analysis results obtained from simulant-reductant interaction tests.**

Test		Offgas analysis results					
		CO <sub>2</sub>	H <sub>2</sub>	NO <sub>x</sub>	N <sub>2</sub> O	N <sub>2</sub>	CO
TI-RA-#1-HCOOH	Peak <sup>a</sup>	33.5	0.00023	6.93	22.1	0.180	0.0075
	Total <sup>b</sup>	117	0.00035	29.4	58.3	1.080	0.0200
TI-RA-#1-Glycolic	Peak <sup>a</sup>	0.350	0.00025	0.470	0.0480	0.160	0.0071
	Total <sup>b</sup>	1.65	0.00048	0.950	0.330	0.300	0.0120
TI-RA-#1-Sugar	Peak <sup>a</sup>	0.0170	0.0034	0.00057	0.0320	0.000	0.000
	Total <sup>b</sup>	0.0660	0.049	0.012	0.340	0.000	0.000
T95-RA-#2-Carbon	Peak <sup>a</sup>	0.00540	0.00160	0.000	0.000	0.815	0.000
	Total <sup>b</sup>	0.0116	0.0258	0.000	0.000	6.16	0.000
T95-RA-#2-Starch	Peak <sup>a</sup>	0.00440	0.0158	0.000	0.000	0.0714	0.000
	Total <sup>b</sup>	0.0254	0.168	0.000	0.000	0.537	0.000
T95-RA-#2-Citric	Peak <sup>a</sup>	1.29	0.000	0.00060	0.0156	0.196	0.0380
	Total <sup>b</sup>	5.15	0.000	0.0028	0.106	0.901	0.0600

<sup>a</sup> Peak production rate values given in units of mmoles/min.

<sup>b</sup> Total production values given in units of mmoles.

Table 4.3.1.2 contains data summarizing the distribution of Re between the slurry supernate and suspended solids before and after the addition of reductant. According to these data, only about 50% of the rhenium is in the supernate of the simulant prior to reductant addition (the target amount is 3170 mg/L or 0.017M). This indicates that a large portion of the ReO<sub>4</sub><sup>-</sup> has precipitated as a non-soluble salt under conditions encountered in the DSSF simulant. When HCOOH is added to the slurry (10.3 moles per liter) and the mixture boiled, a clear light lavender solution is produced without a precipitate and the solution was determined to be fully loaded with rhenium. Glycolic acid addition (3.43 moles per liter) under the same condition results in an apple green solution that includes a small amount of brown precipitate and again most of the rhenium is found to be in solution. Addition of sugar (0.468 moles per liter) on the other hand does not modify the appearance of the simulant and has little effect on the rhenium content. Activated

**Table 4.3.1.2. Summary of the distribution of Re between the slurry supernate and suspended solids before and after the addition of reductant.**

Test	Reductant	Re concentration (mg/L)		
		Before addition of reductant	After addition of reductant	Condenser
TI-RA-#1-HCOOH	formic acid	1500±150	3500±350	NM
TI-RA-#1-Glycolic	glycolic acid	1440±144	3000±300	NM
TI-RA-#1-Sugar	sugar	1410±141	1800±180	NM
T95-RA-#2-Carbon	carbon black	NM	810±81	0.037±0.004
T95-RA-#2-Starch	corn starch	NM	1540±154	0.53±0.05
T95-RA-#2-Citric	citric acid	NM	2220±222	0.57±0.06

NM = not measured.

charcoal appears to reduce the rhenium concentration in solution perhaps by adsorption. Citric acid only moderately increases the rhenium content while causing little change in the appearance of the simulant. Starch addition under these conditions results in a viscous, shear-thickening greenish liquid that gels as it cools. Samples of refluxing condensate from the last three of the six tests were analyzed for rhenium and these analyses suggest that very little rhenium was being transported in the gas stream (e.g., as a aerosol).

#### 4.3.2. DSSF/Glass Precursor-Reductant Interactions with Glass Precursors

4.3.2.1 Citric, Glycolic, and Formic Acids. These organic acids were chosen because they have been previously utilized in HLW treatment, they span a wide range of reducing capacity, and they can modify the waste slurry properties such as pH and total dissolved solids which influences the slurry rheology. Figures 4.3.2.1.1, 4.3.2.1.2, and 4.3.2.1.3 show the temperature and offgas profiles as a function of time which resulted from drying the melter feeds containing the three organic acids. In all three cases the peak offgas generation rate coincided with the period of most rapid temperature increase, indicating that they are both the result of exothermic chemical denitration reactions. Both the glycolic and citric acid containing feeds exhibited very rapid and strong exotherms (in excess of 500°C). The formic acid containing feed displayed a more subdued exotherm which lasted about 45 minutes.

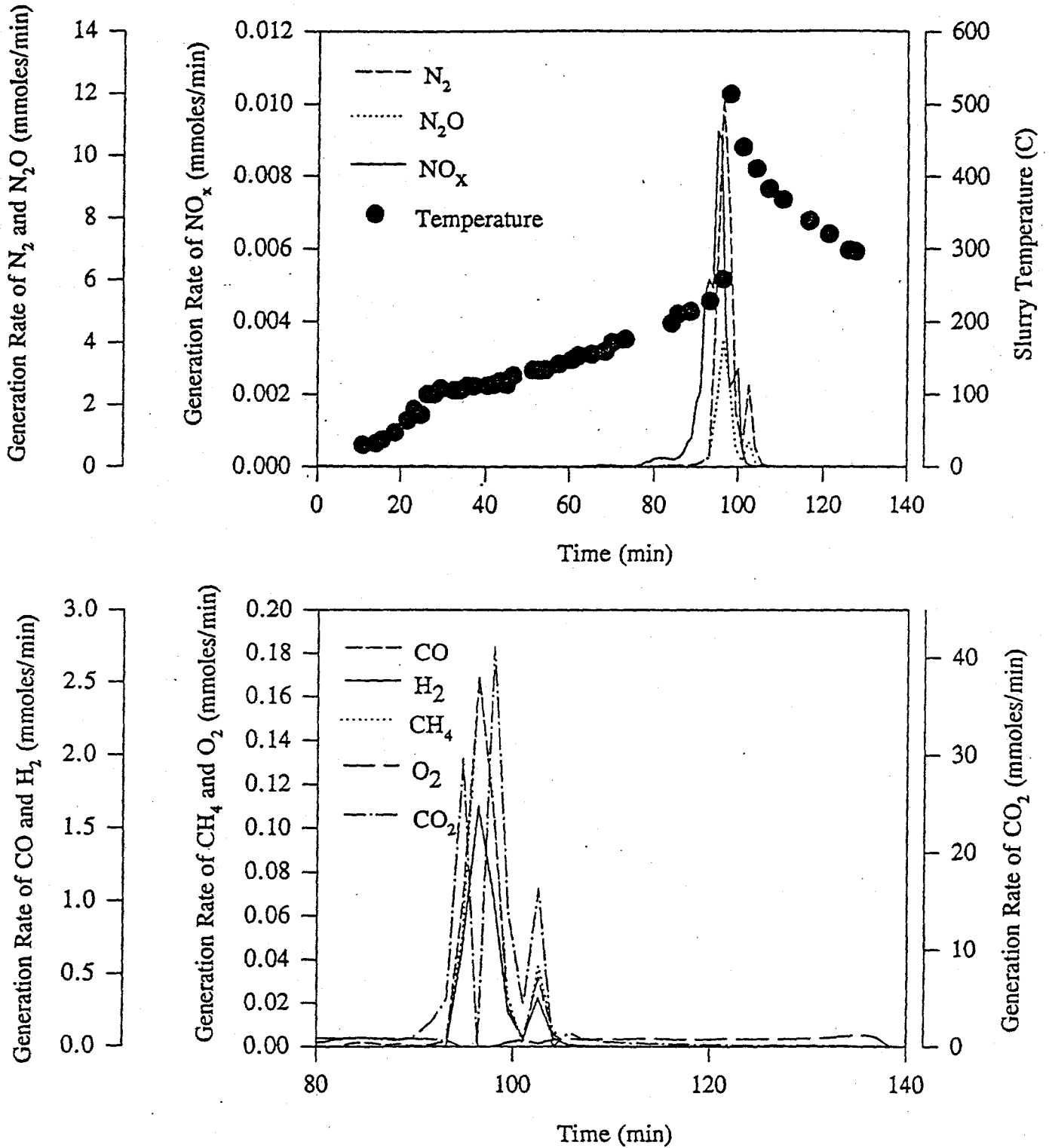


Figure 4.3.2.1.1. Temperature and offgas profiles as a function of time which resulted from drying the melter feed containing citric acid.

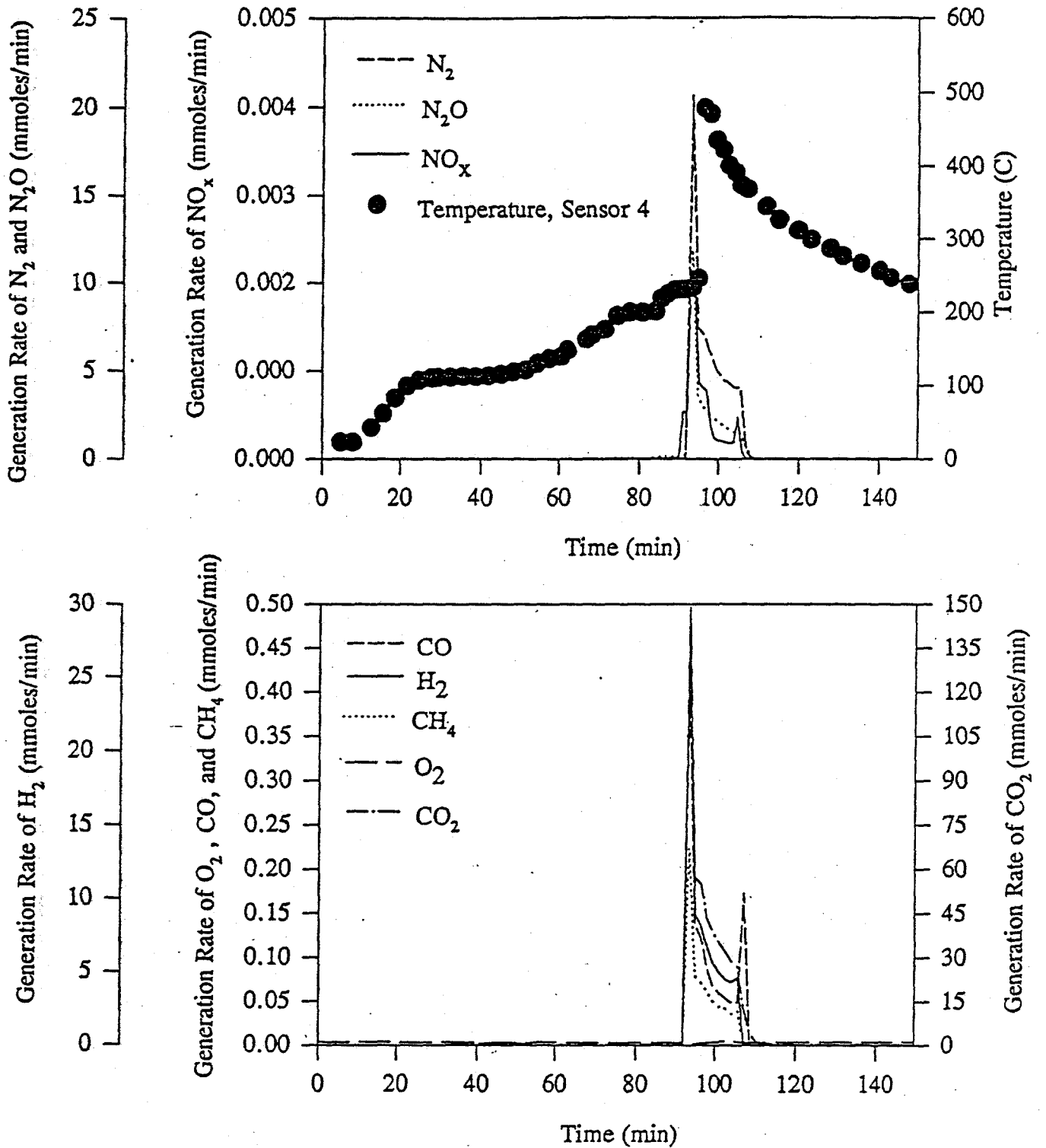


Figure 4.3.2.1.2. Temperature and offgas profiles as a function of time which resulted from drying the melter feed containing glycolic acid.

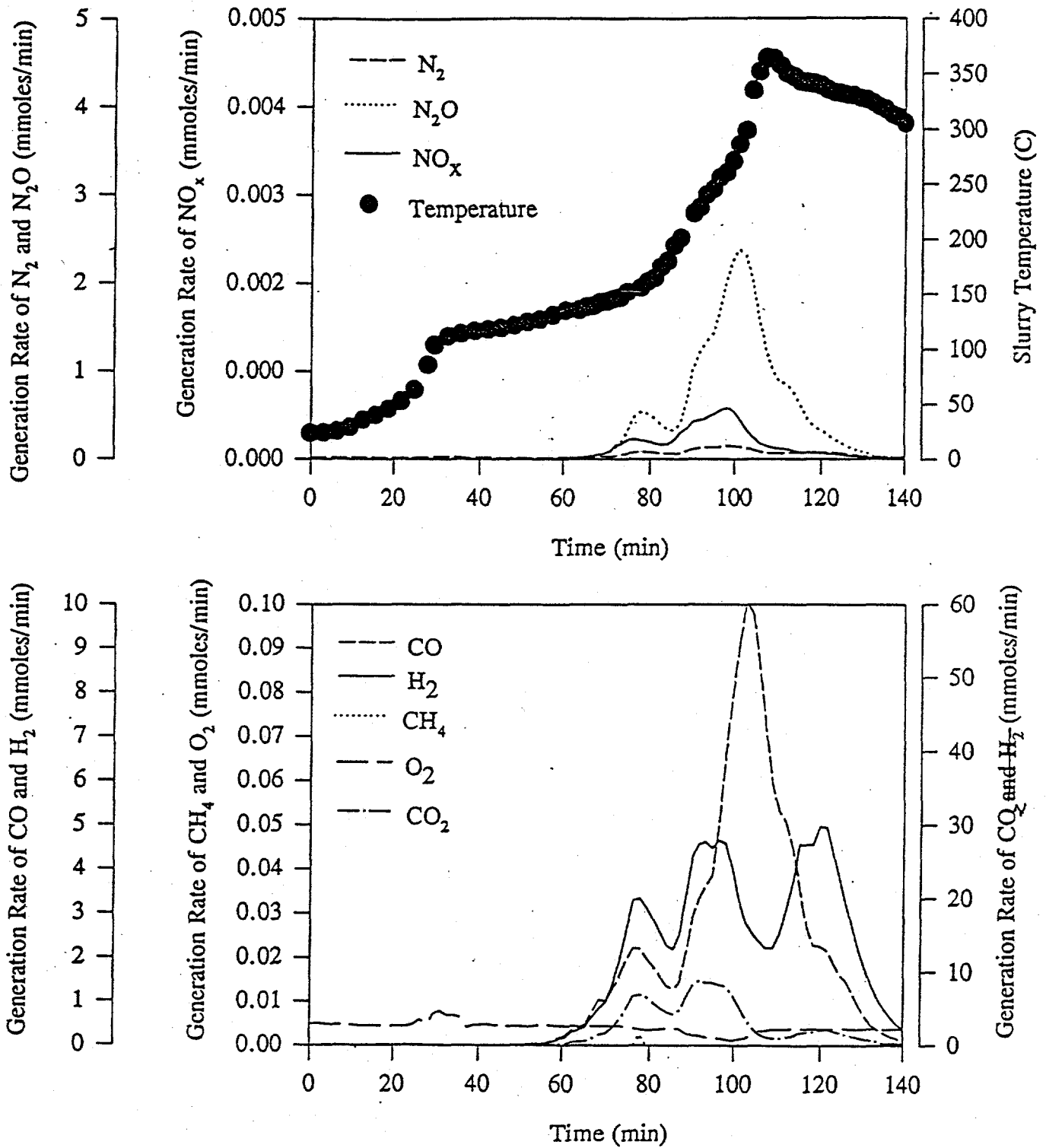


Figure 4.3.2.1.3. Temperature and offgas profiles as a function of time which resulted from drying the melter feed containing formic acid.

The offgas generation characteristic of each exotherm is given in Table 4.3.2.1.1. The peak generation rates computed from results obtained from a rapid (energetic) exotherm have an unknown but significant potential for error because the sampling rates for gases measured with the GC and FTIR are relatively slow compared to the exothermic reaction rate which could be completed in less than a minute. However the ratio of gases measured on the GC would be correct if the reactions producing them occur over the same time span. Keeping these caveats in mind, the following conclusions can be made: 1) citric acid displayed the same offgas pattern as sugar; 2) both formic acid and glycolic acid produced considerable H<sub>2</sub> while formic also produced a relatively large amount of CO; and 3) all of the gas compositions indicated that a considerable portion of the chemical reactions taking place were different from the base relations 3.2.2.1-3.2.2.4, as discussed above.

**Table 4.3.2.1.1. Results of offgas analysis obtained from dry-out/low-temperature calcination tests performed on melter feeds containing formic, glycolic, and citric acids.**

Test		Offgas analysis results						
		CO <sub>2</sub>	H <sub>2</sub>	NO <sub>x</sub>	N <sub>2</sub> O	N <sub>2</sub>	CO	CH <sub>4</sub>
T95-LLW-1-HCOOH	Peak <sup>a</sup>	8.92	4.96	0.60	2.39	0.15	10.07	0.00
	Total <sup>b</sup>	244.97	216.89	14.00	50.36	7.54	228.59	0.01
T95-LLW-1-Glycolic	Peak <sup>a</sup>	146.93	29.78	11.9	11.88	20.64	0.40	0.22
	Total <sup>b</sup>	653.31	121.16	50.10	50.14	101.95	1.86	1.01
T95-LLW-1-Citric	Peak <sup>a</sup>	41.15	1.35	9.2	4.1	12.02	2.54	0.17
	Total <sup>b</sup>	202.07	6.37	53.7	18.04	53.23	9.62	0.62

<sup>a</sup> Peak production rate values given in units of mmoles/min.

<sup>b</sup> Total production values given in units of mmoles.

Ammonia generation was monitored during the tests by directing a known fraction of the offgas through an acidified bubble trap solution. These results are presented in Table 4.3.2.1.2. The amount of NH<sub>3</sub> generated by the dry-out and low temperature calcination of the melter feed slurry was calculated from the volume of trap solution, the change in NH<sub>3</sub> concentration over the representative time period, and the estimated fraction of off-gas flow passing through the bubble trap solution. An average generation rate was calculated by dividing the amount generated during a period by the length of the period. Note that the amount of ammonia added as

**Table 4.3.2.1.2. Results of NH<sub>3</sub> offgas analysis obtained from dry-out/low-temperature calcination tests performed on melter feeds containing formic, glycolic, and citric acids.**

Test		NH <sub>3</sub>
T95-LLW-1-HCOOH	Peak <sup>a</sup>	1.49
	Total <sup>b</sup>	129.85
T95-LLW-1-Glycolic	Peak <sup>a</sup>	1.85
	Total <sup>b</sup>	32.61
T95-LLW-1-Citric	Peak <sup>a</sup>	64.21
	Total <sup>b</sup>	998.40

<sup>a</sup> Peak production rate values given in units of mg/min.

<sup>b</sup> Total production values given in units of mg.

ammonium perrhenate is about 0.289 g of NH<sub>3</sub> per liter for tests containing rhenium, so the average test using about 0.2 L of simulant would include 57.8 mg of NH<sub>3</sub> from this source. Only the feed treated with glycolic acid produced less NH<sub>3</sub> than the originally shimmed amount. The HCOOH containing feed produced the next smallest amount, evolving twice as much NH<sub>3</sub> as was shimmed. However, HCOOH and glycolic acid containing feeds evolved more H<sub>2</sub> than the sugar containing feeds (see below). On the other hand, all of the feeds containing sugar as a reductant produced significantly more NH<sub>3</sub> including the one USBM dried feed that was evaluated.

Table 4.3.2.1.3 summarizes the analytical results for rhenium in primary and secondary condensates collected during the dry-out/low temperature calcination tests conducted using the different reductants at various concentrations. The "primary" data are rhenium analyses of primary condenser composite samples taken during the test. Occasionally a second container was started and this is represented by the second analysis given for a particular test ("secondary"). The observation that the concentration of Re in the second condenser is always higher than that of the first may be explained by the fact that the former represents condensate taken near the end of the drying period and during any exothermic activity after the dry-out. Aerosol formation, formation of trace amounts of more volatile rhenium compounds or simple volatilization of the rhenium compounds present would be the chief Re transport mechanisms that would deliver Re to the

**Table 4.3.2.1.3. Summary of the distribution of Re between the primary and secondary condensers after the dry-out/low temperature calcination of various melter feeds.**

Test	Re concentration (mg/L)	
	Primary condenser	Secondary condenser
T95-LLW-1- HCOOH	0.37 0.30	0.42 3.80
T95-LLW-1- Glycolic	NM	NM
T95-LLW-1- Citric	0.25 4.90	8.8

NM = not measured.

condensers. The formation of aerosols (fog in the reaction chamber, through the condensers, and out to the ammonia trap) observed in many of the tests performed makes this mechanism the most likely explanation.

4.3.2.2. Sugar, Starch, and Carbon. The following discussion focused on sugar because only a limited number of tests were performed using starch and carbon, which presented experimental difficulties related to wetting (carbon) and feed thickening (starch). Sugar, starch, or carbon are the cheapest, most environmentally benign reductants that could be applied to the destruction of nitrates and nitrites. Ideally they result in the "black powder" reactions given by relations 3.2.2.1-3.2.2.4 above.

Focusing on sugar, Figures 4.3.2.2.1, 4.3.2.2.2, 4.3.2.2.3, and 4.3.2.2.4 illustrate the time-temperature-off-gas profiles typically observed when sugar is used as a reductant in the LLW simulant. Refer to Table 4.1.1 for information regarding the ratio of reductant to oxidant. Note that two levels of nitrate-nitrite loading were also investigated which will be discussed below. As with the other reductant systems, the offgas is almost totally evolved during the exothermic event. For sugar the exotherm occurs at about 270°C resulting in a temperature spike and a rush of offgas which pressurizes the reaction vessel to a few psig. The exothermic event with sugar is over in less than a minute, but it takes several more minutes for the off-gas system to detect and the system to be flushed by the sweep gas. Thus, the broadening

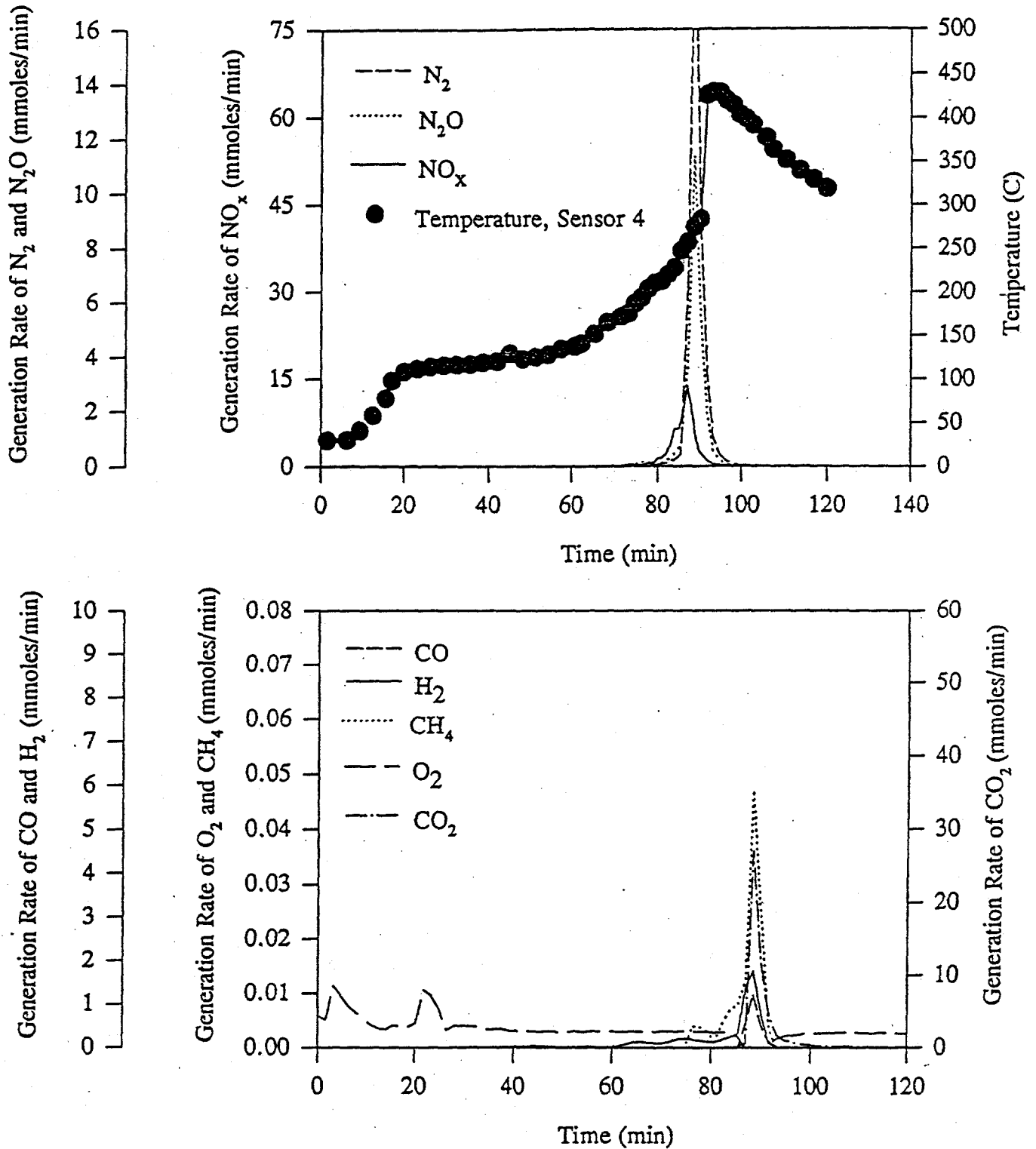


Figure 4.3.2.2.1. Temperature and offgas profiles as a function of time which resulted from the T95-LLW-Sugar(0.5) test.

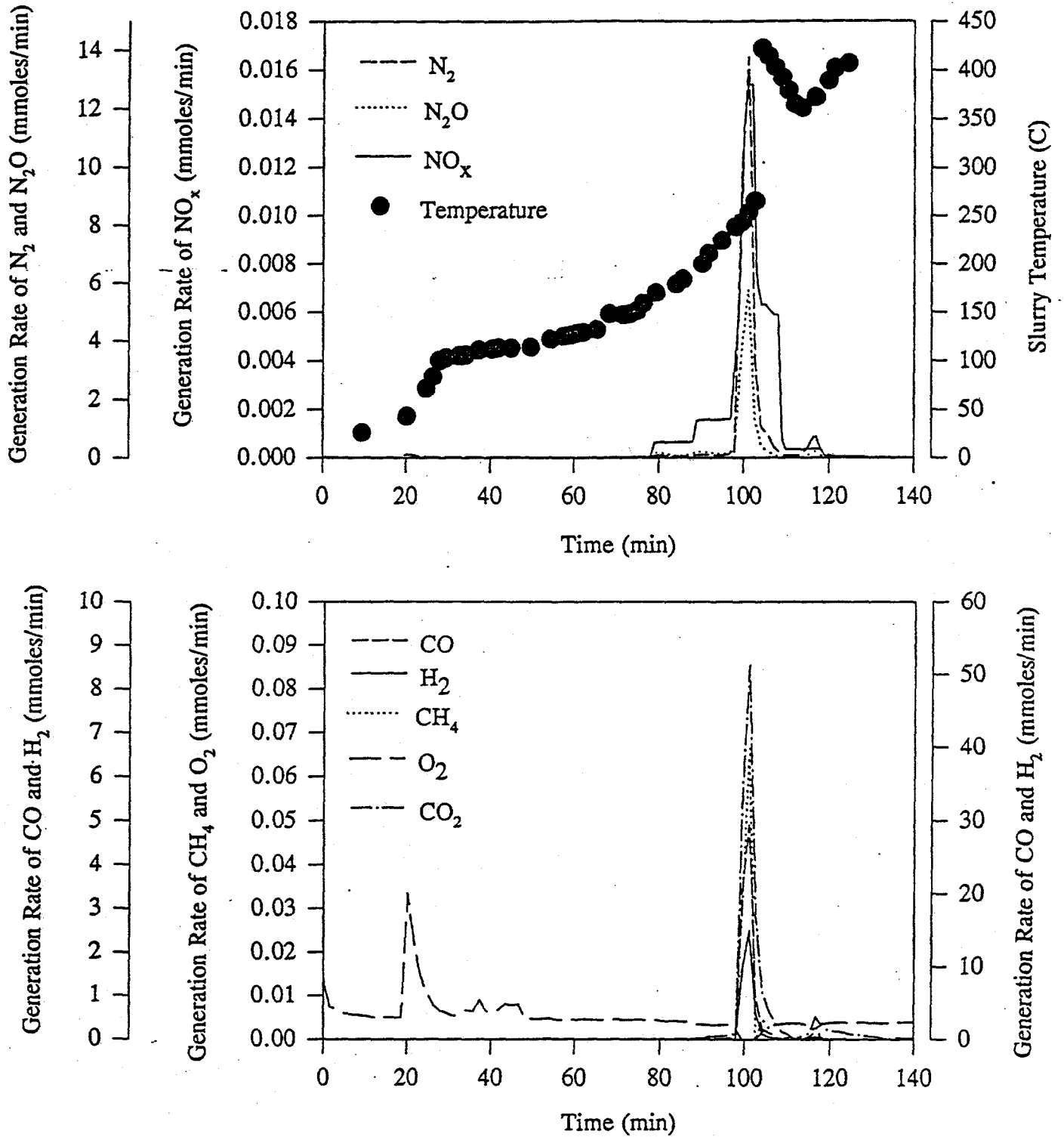


Figure 4.3.2.2.2. Temperature and offgas profiles as a function of time which resulted from the T95-LLW-Sugar(1.0) test.

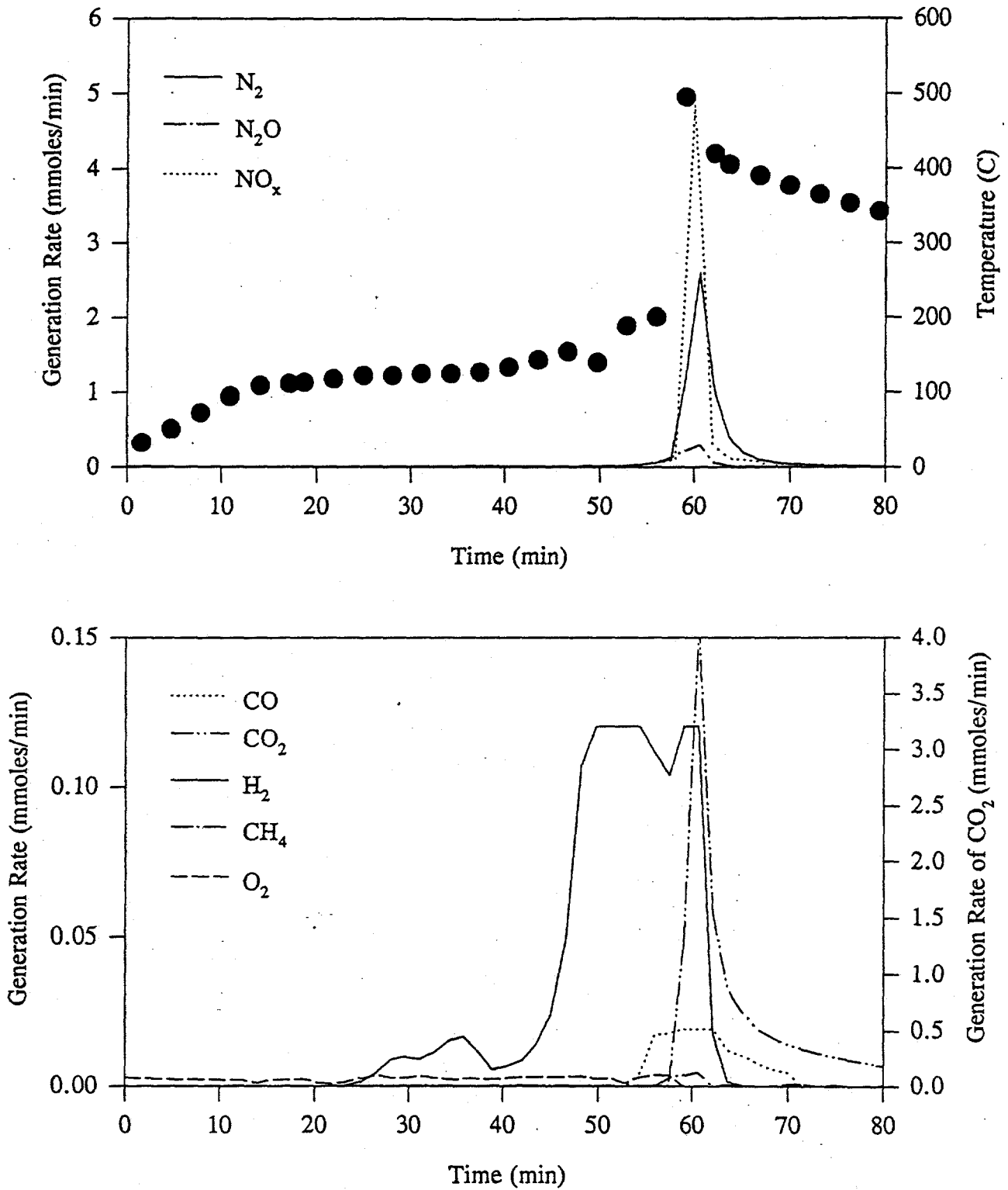


Figure 4.3.2.2.3. Temperature and offgas profiles as a function of time which resulted from the T95-SLLW-Sugar(0.5) test.

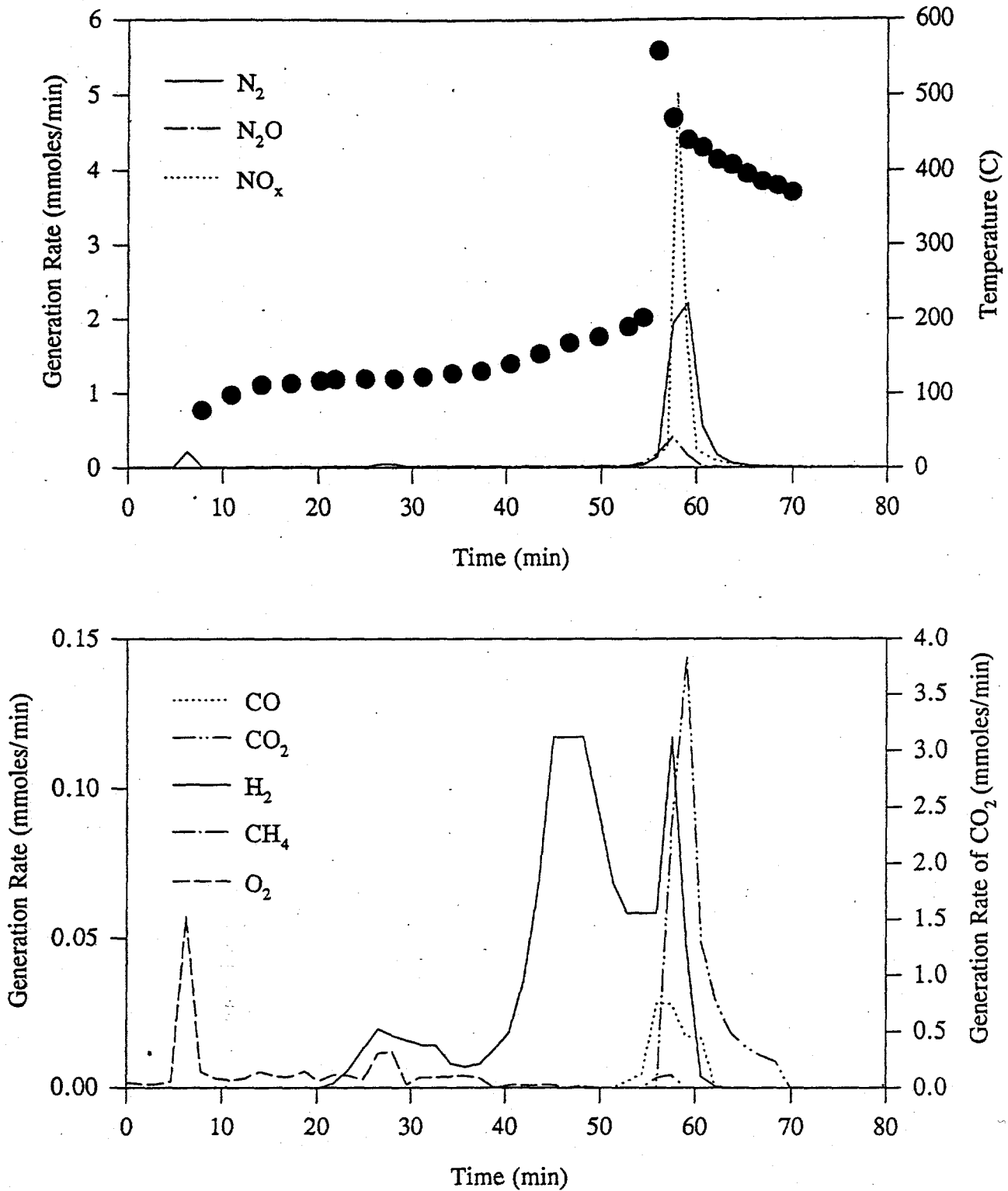


Figure 4.3.2.2.4. Temperature and offgas profiles as a function of time which resulted from the T95-SLLW-Sugar(0.75) test.

of the offgas peaks with respect to time observed for this system is not representative of the true rate of reaction. The total amount of offgas appears to vary considerably from test to test, but it is not known how much of this variation is due to the saturation of the off-gas detection system during the exotherm spike and how much is due to differences in reaction routes in the systems tested.

The offgas totals given in Table 4.3.2.2.1 show again that the "black powder" reactions appear to result in a significant contribution (i.e., abundant CO<sub>2</sub> and N<sub>2</sub> but low CO), but that alternate reaction routes are also indicated (i.e., abundant amounts

**Table 4.3.2.2.1. Results of offgas analysis obtained from dry-out/low-temperature calcination tests performed on melter feeds containing sugar and starch.**

Test		Offgas analysis results						
		CO <sub>2</sub>	H <sub>2</sub>	NO <sub>x</sub>	N <sub>2</sub> O	N <sub>2</sub>	CO	CH <sub>4</sub>
T95-LLW-1-Sugar	Peak <sup>a</sup>	42.29	5.64	5.12	4.38	10.18	4.61	0.15
	Total <sup>b</sup>	193.40	23.90	22.00	18.00	40.00	19.20	0.59
T95-LLW-2-Sugar(1.0)	Peak <sup>a</sup>	51.20	2.49	6.20	5.77	13.77	4.90	0.07
	Total <sup>b</sup>	209.31	8.53	97.20	22.76	53.86	16.63	0.17
T95-LLW-2-Sugar(0.5)	Peak <sup>a</sup>	27.00	1.78	13.67	11.39	20.81	1.24	0.05
	Total <sup>b</sup>	78.66	11.19	71.22	40.68	68.59	3.92	0.18
T95-LLW-Sugar(0.75)	Peak <sup>a</sup>	11.50	1.60	6.00	5.10	11.90	0.30	0.00
	Total <sup>b</sup>	38.20	5.50	31.50	19.20	44.80	0.90	0.10
T95-LLW-Starch(1.0)	Peak <sup>a</sup>	60.58	15.68	5.04	8.70	29.25	10.78	0.21
	Total <sup>b</sup>	116.44	28.84	14.60	19.22	56.80	17.59	0.35
T95-SLLW-Sugar(1.0)	Peak <sup>a</sup>	125.00	15.00	7.41	20.60	71.00	0.014	0.40
	Total <sup>b</sup>	270.00	30.00	34.20	43.00	150.00	0.0558	0.80
T95-SLLW-Sugar(0.75)	Peak <sup>a</sup>	25.60	1.30	5.00	4.70	21.50	0.30	0.00
	Total <sup>b</sup>	51.20	3.60	8.60	8.60	39.70	0.50	0.00
T95-SLLW-Sugar(0.5)	Peak <sup>a</sup>	35.70	3.40	4.80	6.40	32.40	0.50	0.10
	Total <sup>b</sup>	75.30	7.10	12.00	11.50	60.70	0.90	0.20

<sup>a</sup> Peak production rate values given in units of mmoles/min.

<sup>b</sup> Total production values given in units of mmoles.

of  $\text{NO}_x$ ,  $\text{N}_2\text{O}$ ,  $\text{H}_2$  were also detected). The ratio of reductants to oxidants in the simulant affected the ratio of  $\text{NO}_x$  to  $\text{N}_2$  produced during the exothermic reaction. The differences in the simulants is due to the hydroxide to nitrate-nitrite ratio which would influence the composition of the salt melt that reacts with the reducing agent (sugar).

All of the sugar tests produced significant amounts of  $\text{NH}_3$  (see Table 4.3.2.2.2). The amounts ranged from about 2.5 to 7 g  $\text{NH}_3$  per liter of simulant. The maximum generation rate of  $\text{NH}_3$ , for those tests where it could be determined, is coincident

**Table 4.3.2.1.2. Results of  $\text{NH}_3$  offgas analysis obtained from dry-out/low-temperature calcination tests performed on melter feeds containing sugar and starch.**

Test		$\text{NH}_3$
T95-LLW-1-Sugar	Peak <sup>a</sup>	13.26
	Total <sup>b</sup>	592.92
T95-LLW-2-Sugar(1.0)	Peak <sup>a</sup>	11.74
	Total <sup>b</sup>	1342.39
T95-LLW-2-Sugar(0.5)	Peak <sup>a</sup>	72.68
	Total <sup>b</sup>	1778.39
T95-LLW-Sugar(0.75)	Peak <sup>a</sup>	14.81
	Total <sup>b</sup>	388.7
T95-LLW-Starch(1.0)	Peak <sup>a</sup>	16.24
	Total <sup>b</sup>	833.93
T95-SLLW-Sugar(1.0)	Peak <sup>a</sup>	NM
	Total <sup>b</sup>	NM
T95-SLLW-Sugar(0.75)	Peak <sup>a</sup>	11.39
	Total <sup>b</sup>	420.9
T95-SLLW-Sugar(0.5)	Peak <sup>a</sup>	29.35
	Total <sup>b</sup>	1164.2

<sup>a</sup> Peak production rate values given in units of mg/min.

<sup>b</sup> Total production values given in units of mg.

NM = not measured.

with the exothermic event (i.e., test T95-LLW-Sugar-0.5). However the results also indicated that lesser amounts of  $\text{NH}_3$  were generated at other times as well (i.e. earlier periods of test T95-LLW-Sugar-0.5).

Table 4.3.2.2.3 summarizes the analytical results for rhenium in primary and secondary condensates collected during the dry-out/low temperature calcination tests conducted using sugar and starch at various concentrations. Rhenium transport was discussed in the previous section and the data for sugar and starch is consistent with the comments made in that section.

**Table 4.3.2.1.3. Summary of the distribution of Re between the primary and secondary condensers after the dry-out/low temperature calcination of melter feeds containing various amounts of sugar and starch.**

Test	Re concentration (mg/L)	
	Primary condenser	Secondary condenser
T95-LLW-1-Sugar	NM	NM
T95-LLW-2-Sugar(1.0)	0.25 0.34	2.04 NM
T95-LLW-2-Sugar(0.5)	0.03 0.56	1.30 NM
T95-LLW-Sugar(0.75)	0.06 0.10	1.70 NM
T95-LLW-Starch(1.0)	<0.03 0.13	0.19 NM
T95-SLLW-Sugar(1.0)	NM	NM
T95-SLLW-Sugar(0.75)	0.94	9.70
T95-SLLW-Sugar(0.5)	1.01	12.50

NM = not measured.

### 4.3.2.3. Vendor Feeds

Figures 4.3.2.3.1 and 4.3.2.3.2 show the time-temperature-offgas generation rate profiles for the USBM-LD6-5510-1400B and USBM-M1BPW-011P tests respectively. These tests were performed on materials that were already dry (test USBM-LD6-5510-1400B) or damp (test USBM-M1BPW-011P). Both tests had strong exotherms initiating between 250°C and 300°C and in both cases essentially all of the offgas evolution occurred in conjunction with the exotherm. The gas evolution patterns and exotherms for the vendor feed are most similar to those obtained from the T95-SLLW-Sugar tests (i.e., for feeds containing target oxidant levels).

Table 4.3.2.3.1 summarizes the results of the offgas analysis obtained from these tests. The NO<sub>x</sub> to N<sub>2</sub> ratios for the two vendor tests were 0.20 and 0.29 respectively which were similar to the T95-SLLW-Sugar tests. Ammonia offgas analysis was performed only during the USBM-M1BPW-011P test and indicated that a total of 395.37 mg NH<sub>3</sub> (3.3g NH<sub>3</sub>/L of feed) was produced with a peak rate occurring at 7.34 mg/min.

Table 4.3.2.3.1. Results of offgas analysis obtained from dry-out/low-temperature calcination tests performed on the USBM melter feed.

Test		Offgas analysis results						
		CO <sub>2</sub>	H <sub>2</sub>	NO <sub>x</sub>	N <sub>2</sub> O	N <sub>2</sub>	CO	CH <sub>4</sub>
USBM-LD6-5510-1400B	Peak <sup>a</sup>	94.90	2.50	4.40	7.90	35.70	2.60	NM
	Total <sup>b</sup>	488.20	16.40	31.80	37.60	156.80	11.50	NM
USBM-M1BPW-011	Peak <sup>a</sup>	59.40	0.21	5.24	6.43	37.00	NM	0.0096
	Total <sup>b</sup>	122.10	1.32	23.00	18.80	78.20	NM	0.010

<sup>a</sup> Peak production rate values given in units of mmoles/min.

<sup>b</sup> Total production values given in units of mmoles.

Ammonium perchlorate was not added during feed preparation at the USBM. Therefore, Re chemical analyses were not performed during these tests.

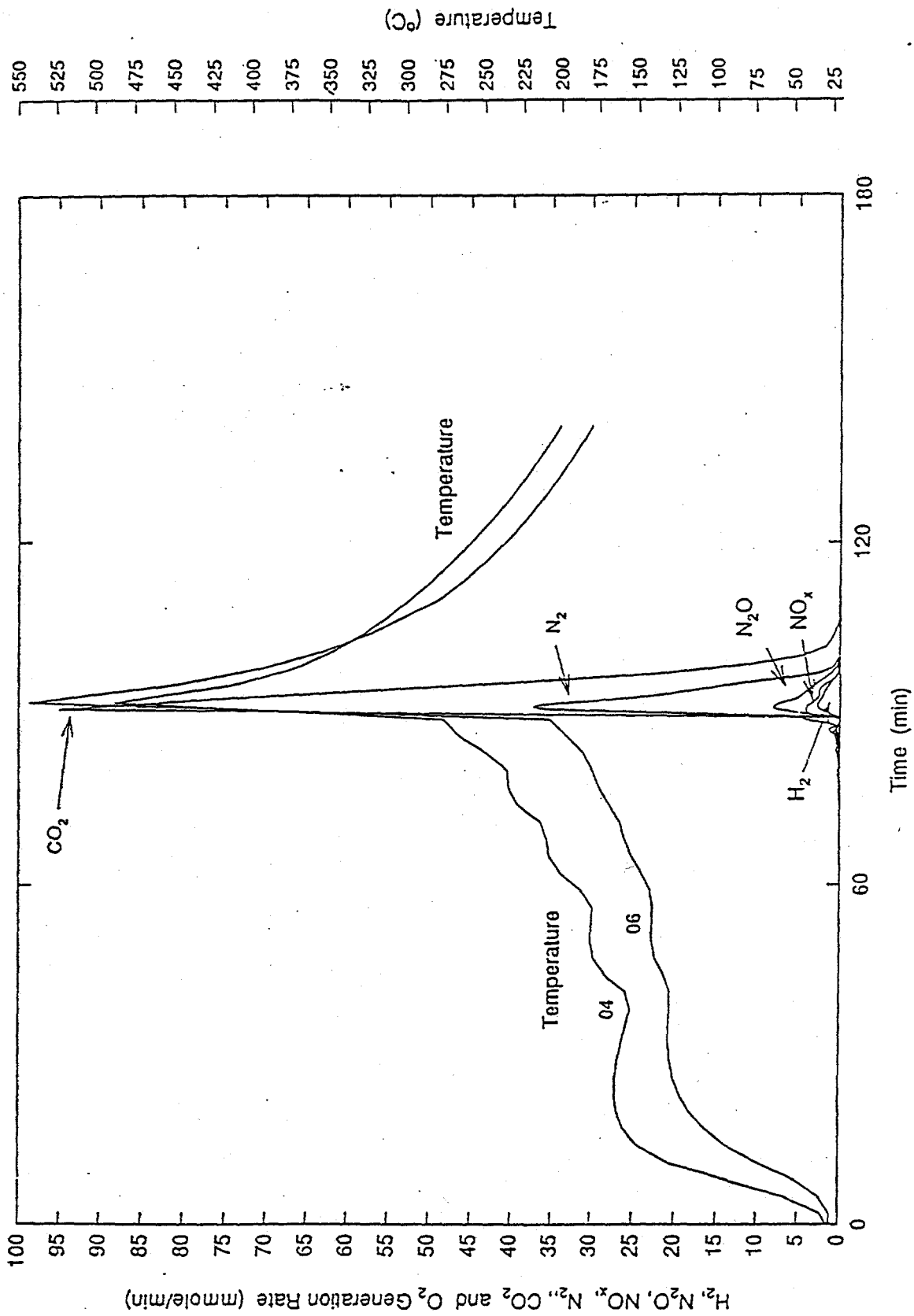


Figure 5.3.1. Temperature and offgas profiles as a function of time which resulted from the USBM-LD6-5510-1400B test.

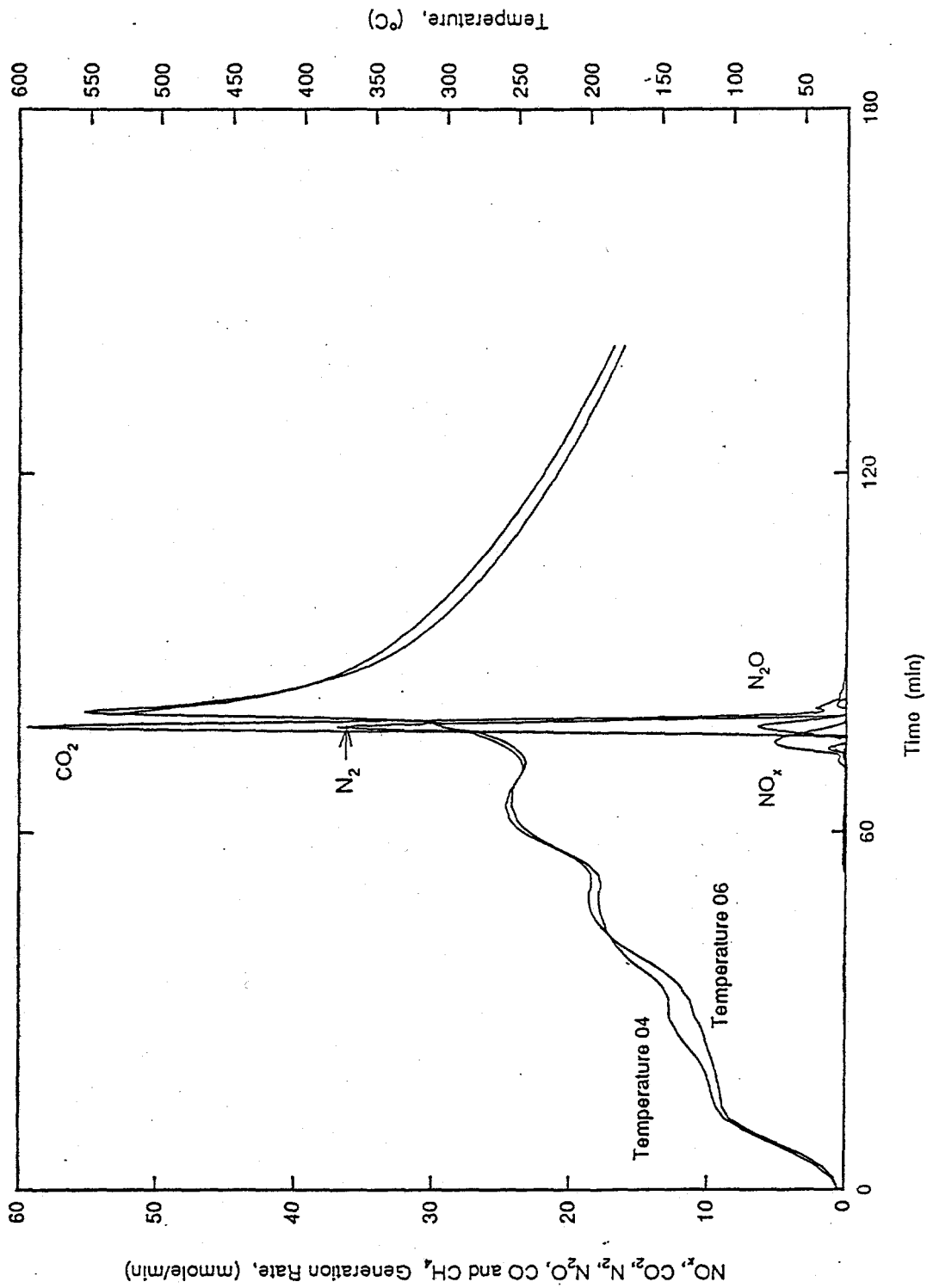


Figure 5.3.2. Temperature and offgas profiles as a function of time which resulted from the USBM-M1BPW-011P test.

## 5. HIGH-TEMPERATURE CALCINATION TEST RESULTS ON THE LLW BASELINE, US BUREAU OF MINES FEED, AND VECTRA FEED

### 5.1. Introduction

To support LLW melter vendor tests, high-temperature calcination tests were performed on the LLW DSSF 10M Na baseline feed, the US Bureau of Mines (USBM) feed, and the Vectra Corporation (Vectra) feed. As in the dry-out/low-temperature calcination tests discussed in Section 4, offgas characteristics will be an important aspect of the tests described here. Furthermore, feed foaming occurs at temperatures above approximately 700°C. Thus, monitoring the degree of foaming during heating is another important issue that will be addressed in this section.

### 5.2. Experimental

The USBM and Vectra feeds were used as-received. The DSSF-based feed was prepared by mixing the DSSF simulant with the appropriate amount of glass precursor additives (see Table 4.2.1.3) and subsequently dried in an oven at 90-120°C for several days.

Each feed was crushed for 2 minutes in an agate disc mill to approximately -120 mesh. A 3-g sample of each crushed feed was transferred to a quartz crucible. Ultrasound was used to remove feed from the crucible sides. Samples were heated at a rate of 10°C/min in the furnace (Figure 5.2.1) from room temperature to 1300°C. The volume expansion of the samples due to foaming was measured from recorded images using a video camera.

Offgas from the heated samples was analyzed by gas chromatography-mass spectrometry (GC-MS) using a Hewlett Packard model 5890 gas chromatograph (GC) and a model 5971 mass spectrometer (MS). The GC's Pora PLOT Q column was maintained at 90°C. The inlet pressure was 6.1 psig and a corresponding backpressure regulator was set at 6.1 psig (to avoid baseline upsets). GC injections of 0.5 mL were made once a minute by a valve rotator. This allowed off-gas species to be identified every 10°C. A sweep gas of 1 wt% He in Ar was used at a flow rate of 250 mL/min. The gases that were measured quantitatively included H<sub>2</sub>, O<sub>2</sub>, CO<sub>2</sub>, CO, NO, N<sub>2</sub>, and CH<sub>4</sub>.

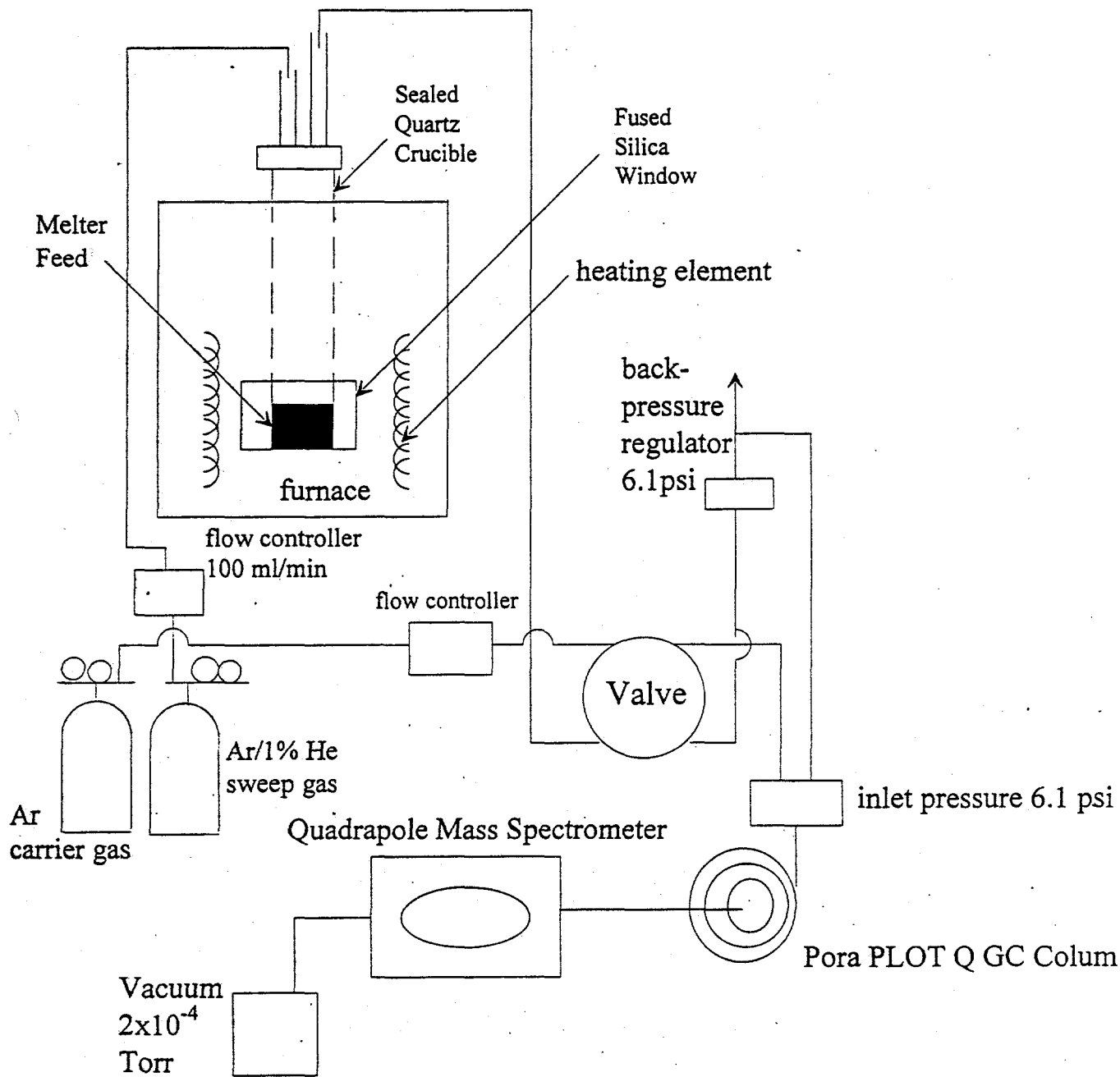


Figure 5.2.1. Schematic diagram of the system used for the high-temperature calcination studies in this work.

### 5.3. Results and Discussion

Figures 5.3.1, 5.3.2, and 5.3.3 show the offgas profiles and the sample's volume expansion as a function of temperature for the DSSF, USBM, and Vectra feeds respectively. Table 5.3.1 summarizes this data in terms of total amount of gas produced and peak gas production rate for each species detected.

**Table 5.3.1. Results of offgas analysis obtained from high-temperature calcination tests performed on DSSF, USBM, and Vectra melter feeds. Maximum volume expansions are also reported.**

Gas	Feed		
	DSSF	USBM	Vectra
	<i>Total (mmoles/g)</i>		
N <sub>2</sub> O	0.12	0.15	0.00
CO <sub>2</sub>	1.56	1.47	3.51
O <sub>2</sub>	0.92	0.02	0.00
NO	0.87	0.23	0.00
CO	0.00	0.21	0.19
N <sub>2</sub>	0.21	1.00	0.06
CH <sub>4</sub>	0.00	0.00	0.00
H <sub>2</sub>	0.15	0.12	0.00
	<i>Peak (mmoles/min/g)</i>		
N <sub>2</sub> O	0.02	0.02	0.00
CO <sub>2</sub>	0.10	0.08	0.18
O <sub>2</sub>	0.06	0.00	0.00
NO	0.04	0.03	0.00
CO	0.00	0.01	0.01
N <sub>2</sub>	0.01	0.08	0.00
CH <sub>4</sub>	0.00	0.00	0.00
H <sub>2</sub>	0.02	0.01	0.00
Volume	2.1	2.2	2.0
Expansion			

In contrast to the DSSF and USBM feeds, the Vectra feed produced no N<sub>2</sub>O, NO, or H<sub>2</sub> offgases up to 1200°C. These results indicate that the nitrate/nitrite in the LLW feed has been completely mitigated by the Vectra feed processing conditions.

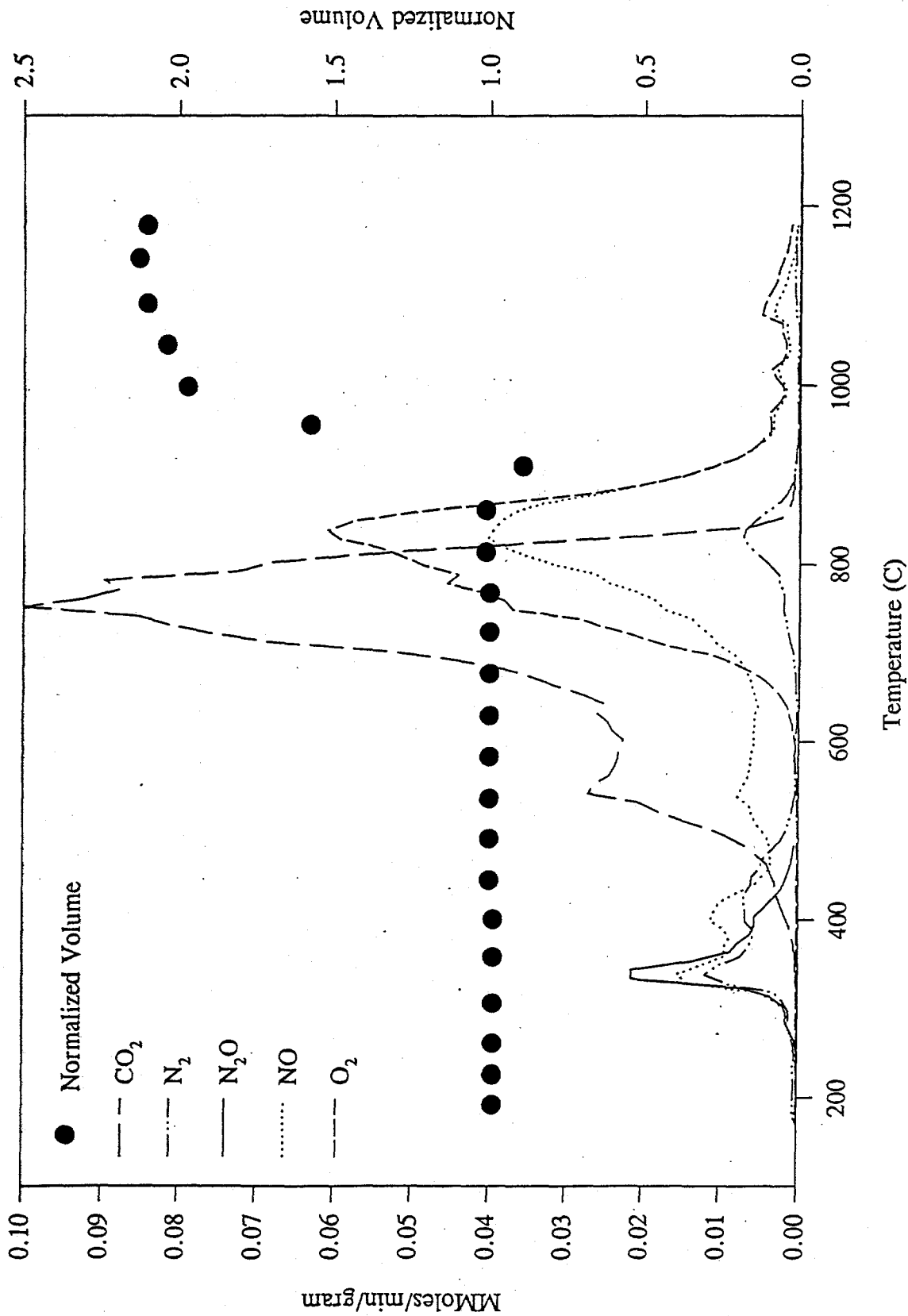


Figure 5.3.1. Offgas profiles and normalized sample volume as a function of temperature which resulted during calcination of the DSSF feed at 10°C/min.

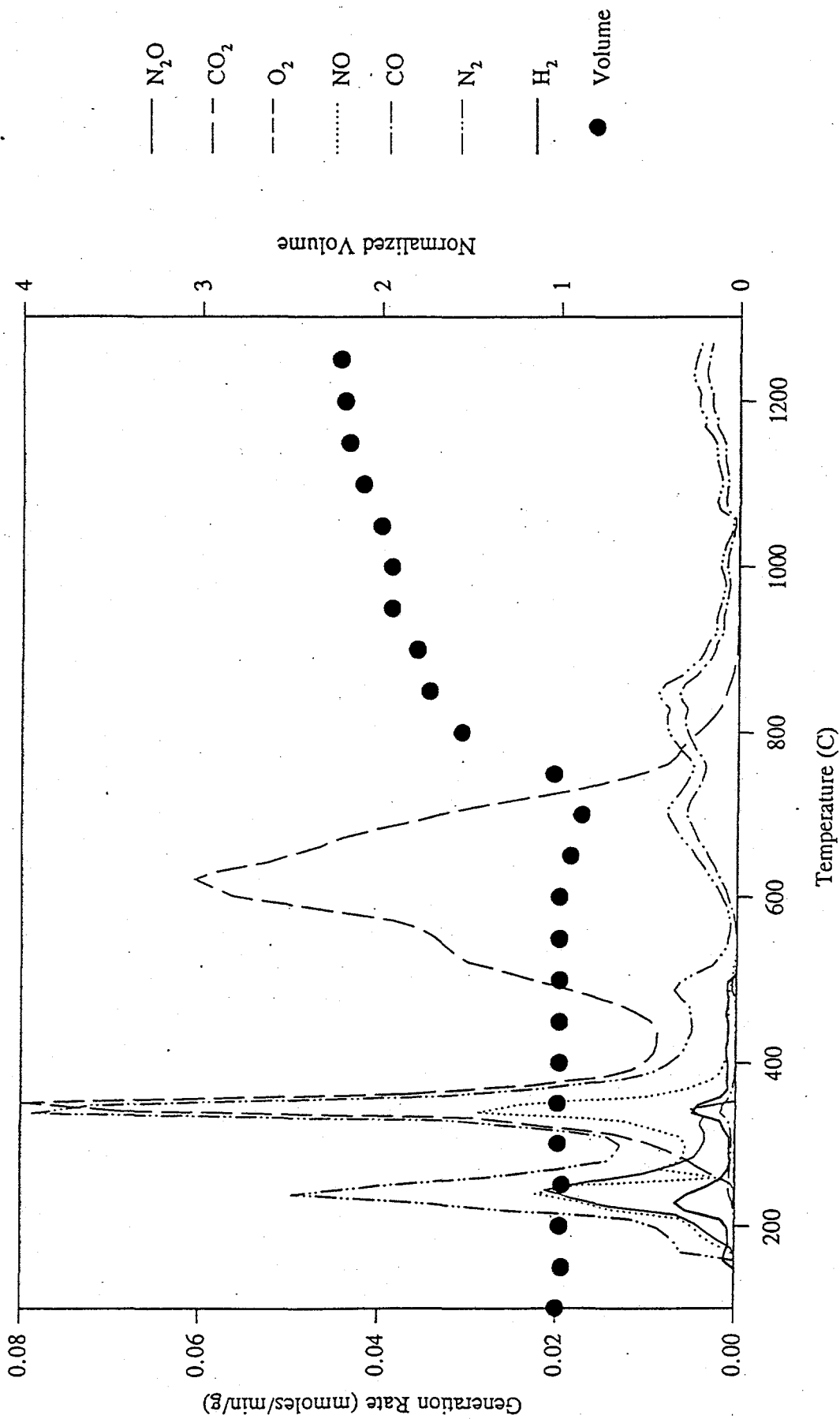


Figure 5.3.2. Offgas profiles and normalized sample volume as a function of temperature which resulted during calcination of the USBM feed at 10°C/min.

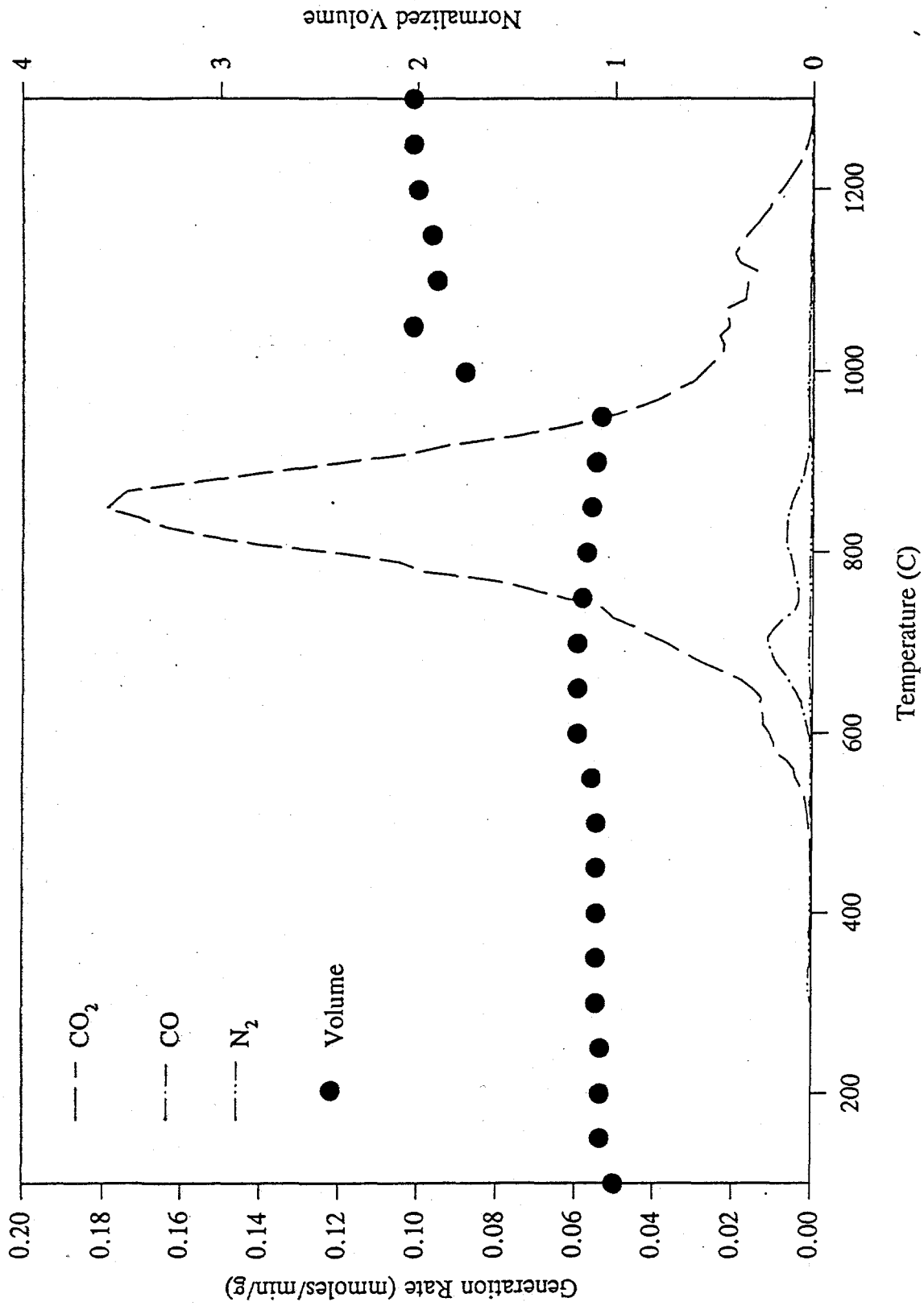


Figure 5.3.3. Offgas profiles and normalized sample volume as a function of temperature which resulted during calcination of the Vectra feed at 10°C/min.

## 6. REFERENCES

- Abe, O., T. Utsunomiya, and Y. Hoshino. 1983. "The Reaction of Sodium Nitrite with Silica." *The Chemical Society of Japan*, 56 p. 428.
- Bond, B.D. and P.W.M. Jacobs. 1966. "The Thermal Decomposition of Sodium Nitrate." *J. Chem Soc. (A)*, p. 1265.
- Bray, L.A. and E.C. Martin. 1962. "Use of Sugar to Neutralize Nitric Acid Waste Liquors." HW-75565, Hanford Atomic Products Operation, Richland, Washington.
- Brickford, D.F., C.J. Coleman, C-L.W. Hsu, and R.E. Eibling. Noble Metal Catalyzed Formic Acid Decomposition, and Formic Acid Denitration. in *Ceramic Transactions Nuclear Waste Management IV*. Ed. G.C. Wicks and D.F. Bickford, Westinghouse Savannah River Co, and L.R. Bunnell, Pacific Northwest Laboratory.
- Burger, L.L., J.L. Ryan, J.L. Swanson, and L.A. Bray. 1973. Salt Waste Volume Reduction by Sodium Removal. BNWL-B-293. Pacific Northwest Laboratory. Richland Washington.
- Burril, K.A. 1987. Chemical Denitration of Aqueous Nitrate Solutions. AECL-9500. Chalk River Nuclear Laboratories. Chalk River, Ontario.
- Cecille, L. and M. Kelm. 1986. "Chemical Reactions Involved in the Denitration Process with HCOOH and HCHO." In *Denitration of Radioactive Liquid Waste*, eds. L. Cecille and S. Halaszovich. Graham & Trotman, Norwell, Massachusetts.
- Chun, K.S. 1977. "Studies on the Thermal Decomposition of Nitrates Found in Highly Active Waste and of Chemicals Used to Convert the Waste to Glass." AERE-R8735. Chemical Technology Division, AERE Harwell.
- Coppinger, E.A. 1963. "Pilot Plant Denitration of Purex Waste with Sugar." HW-77080. Hanford Atomic Products Operation, Richland, Washington.
- Cox, J.L., M.A. Lilga, R.T. Hallen. 1992. Thermochemical Nitrate Reduction. PNL-8226. Pacific Northwest Laboratory. Richland, Washington.
- Evans, T.F. 1959. "The pilot plant denitration of purex wastes with formaldehyde." HW-58587, Hanford Atomic Products Operation, Richland, Washington.
- Forsman, R.C., and G.C. Oberg. 1963. *Formaldehyde Treatment of Purex Radioactive Wastes*. HW-79622, Hanford Atomic Products Operation, Richland, Washington.
- Gass, W.R., S.V. Dighe, and D.F. McLaughlin. 1993. *Plasma Calcination of Simulated High-Level Waste*. 93-9TD3-CALCI-R1. Westinghouse Hanford Company, Richland, Washington.

- Holze, K. H. Finke, M. Kelm, and W. Deckwer. 1979. "Reaction Model for Denitration with Formic Acid of Waste Effluents from Nuclear Fuel Reprocessing Plants." *Chem. Eng.* 2.
- Hoshino, Y., T. Utsunomiya, and O. Abe. 1981. "The Thermal Decomposition of Sodium Nitrate and the Effects of Several Oxides on the Decomposition." *The Chemical Society of Japan*, 54 p. 1385.
- Kelm, M. B. Oser, S. Drobnik, and W.D. Deckwer. 1980. "Denitration of Aqueous Waste Solutions from the Nuclear Fuel Reprocessing." *Nuclear Technology*. 51, pg 27-32.
- Kozlowski, T.R. and R.F. Bartholomew. 1968. "Reactions Between Sodium Carboxylic Acid Salts and Molten Sodium Nitrate and Sodium Nitrite." *Inorg. Chem.* 7:2247.
- Kubota, M, I. Yamaguchi, and H. Nakamura. 1979 "Effects of Nitrite on Denitration of Nuclear Fuel Reprocessing Waste with Organic Reductants." *Journal of Nuclear Science and Technology*, 16 (6).
- MacDougall, C.S., C.K. Bayne, and R.B. Roberson. 1982. "Studies on the Reaction of Nitric Acid and Sugar." *Nuclear Technology*. 58 pg 47-52.
- Meile, L.J. and A.J. Johnson. 1983. *Waste Generation Reduction -- Nitrates FY 1983 Status Report*. RFP-3619, DOE/TIC-4500 (Rev. 72), Rockwell International, Golden, Colorado.
- Newby, B.J. and Dickerson, 1972. E.S. ICP-1008, USAEC.
- Orebaugh, E.G. 1976. "Denitration of Savannah River Plant Waste Streams." DP-1417, E.I. DuPont de Nemours and Company, Aiken, South Carolina.
- Quin, J.P. 1911. *Mellor's Comprehensive Treatise on Inorganic and Theoretical Chemistry*, Vol II, Suppl. II. Wiley and Sons, New York.
- Ray, J.D., and R.A. Ogg, Jr. 1956. "A New Method of Preparing Nitric Oxide." *J. Am. Chem. Soc.* 78:5993.
- Rode, T.V., and G.A. Golder. 1956. "Compounds of Constant and of Variable Composition in the Sodium Superoxide- Sodium Oxide System." *Chemical Abstracts* 50, 12621e, 1956.
- Ryan, J.L. 1994. "Redox Reactions and Foaming in Nuclear Waste Glass Melting." PVTD-C94-03.02C. Pacific Northwest Laboratory. Richland, Washington.

**APPENDIX MATERIAL**









Sample	CO2	H2	Offgas Analyses - All values in mmoles or mmoles per min.			CO	CH4	NH3-mg/min
			NOx	N2O	N2			
T95-LLW-2-SUGAR(1.0)	Peak Rate Total 209.31 sugar added	51.2 2.49 9.53 37.8 g	0.01 0.09	5.77 22.76	13.77 53.86	4.9 18.63	0.07 0.17	
Simulant mass 300 g								
sample	density							
SUGAR(1.0)-2								
SUGAR(1.0)-2a								
SUGAR(1.0)-2S								
Sample								
SUGAR(1.0)-NH3-1	Fraction of Ammon Flow Rate							
SUGAR(1.0)-NH3-2	Iraco Vol./wt. NH3							
SUGAR(1.0)-NH3-3	Iraco Vol./wt. NH3							
SUGAR(1.0)-NH3-4	Iraco Vol./wt. NH3							
SUGAR(1.0)-NH3-5	Iraco Vol./wt. NH3							
SUGAR(1.0)-NH3-6	Iraco Vol./wt. NH3							
Sample								
Primary Condensate	Water Loss Log							
Primary Condensate	Time period amount							
Primary Condensate	10:10-10:20							
Primary Condensate	10min							
Primary Condensate	10min							
Primary Condensate	10min							
Primary Condensate	10min							
Primary Condensate	10min							
Primary Condensate	60min							
Secondary Condensate	all							
T95-LLW-2-SUGAR(0.5)	Peak Rate Total 78.66 sugar added	27 1.78 11.19 18.91 g	13.67 1.78	11.39 40.68	20.81 68.59	1.24 3.92	0.05 0.18	
Simulant mass 300 g								
sample	density							
SUGAR(0.5)-1-1-1(1)								
SUGAR(0.5)-1-1-1(2)								
SUGAR(0.5)-1-1-1(1s)								
Sample								
SUGAR(0.5)-NH3-1	Fraction of Ammon Flow Rate							
SUGAR(0.5)-NH3-2	Iraco Vol./wt. NH3							
SUGAR(0.5)-NH3-3	Iraco Vol./wt. NH3							
SUGAR(0.5)-NH3-4	Iraco Vol./wt. NH3							
SUGAR(0.5)-NH3-5	Iraco Vol./wt. NH3							
SUGAR(0.5)-NH3-6	Iraco Vol./wt. NH3							
Sample								
Primary Condensate	Water Loss Log							
Primary Condensate	Time period amount							
Primary Condensate	10:10-10:20							
Primary Condensate	10min							
Primary Condensate	10min							
Primary Condensate	10min							
Primary Condensate	10min							
Primary Condensate	60min							
Secondary Condensate	all							











